NATIONAL AERONAUTICS AND SPACE ADMINISTRATION

Technical Report 32-1214

Fabrication of the 23-ft Collimating Mirror for the JPL 25-ft Space Simulator

R. P. Eddy

M. R. Heilig

JET PROPULSION LABORATORY

CALIFORNIA INSTITUTE OF TECHNOLOGY

PASADENA, CALIFORNIA

December 15, 1967

NATIONAL AERONAUTICS AND SPACE ADMINISTRATION

Technical Report 32-1214

Fabrication of the 23-ft Collimating Mirror for the JPL 25-ft Space Simulator

R. P. Eddy

M. R. Heilig

Approved by:

George G. Goranson

G. G. Goranson, Manager
Space Simulators and Facility Engineering Section

JET PROPULSION LABORATORY
CALIFORNIA INSTITUTE OF TECHNOLOGY
PASADENA, CALIFORNIA

December 15, 1967

PRECEDING PAGE BLANK NOT FILMED.

Acknowledgments

The fabrication of this 23-ft diam mirror for the JPL solar simulator is an important state-of-the-art development. The authors express their thanks to the following companies and personnel for their contributions: Westinghouse Electric Corp., Sunnyvale (Calif.) Division, weldment fabrication; Pyromet Corp., San Carlos, Calif., heat treatment and creep sagging; Kaiser Aluminum and Chemical Sales, Inc., Los Angeles, data and consultant services; Electroforms, Inc., Los Angeles, electroplating; Tinsley Laboratories, Inc., Berkeley, Calif., grinding and polishing; and Paxton Trucking Company, Los Angeles, transportation.

PRECEDING PAGE BLANK NOT FILMED.

Contents

I. **Introduction** 1

II. **Design Criteria** 1

III. **Design Selection** 2

A. Optical Design 2

B. Structural Design 3

C. Thermal Design 5

IV. **Fabrication Techniques** 7

A. Fabricating the Weldment 7

B. Initial Figuring of Mirror 14

C. Plating the Mirror 16

D. Grinding and Polishing 17

V. **Transportation and Installation** 18

VI. **Aluminizing the Mirror** 21

VII. **Conclusions** 21

References 21

Table

1. Pressure drops in mirror temperature control system 7

Figures

1. Uniformity vs diameter of defect for 1-deg half-angle 2
2. Uniformity vs gaps for 1-deg half-angle 3
3. The 60-deg webbed, geodesic rib structure supporting continuous plate 4
4. Results of deflection vs weight study 5
5. Gas heat-exchange tube 5
6. Aluminized Mylar insulation 6
7. Temperature gradient between mirror and structure vs temperature rate change for modified test model and mirror . . . 6

Contents (contd)

8. Total flow vs tube diameter 7
9. Fabrication specifications 8
10. Bolting preshaped plates to welding fixture 10
11. Welding front face through surface back 11
12. Machining by 40-ft boring mill 11
13. Welding ribs to back of front face plates 12
14. Cooling coils welded inside each rib cell 13
15. Unloading mirror for creep-sagging weldment 13
16. Mirror loading scheme 13
17. Sandbags used to stress center of mirror 14
18. Temperature-creep curves (10–12%) used for stress operations . . . 14
19. Inspection after final machining 15
20. Grind and polish machine suspension 16
21. Figuring mirror with 12-ft ring grinder 16
22. Lapping tool 17
23. Mirror after final polishing 18
24. Most commonly used shipping position. 19
25. Mirror arriving at JPL 19
26. Air tent 19
27. Heliarc welding tube joints 19
28. Moving mirror onto handling cart 20
29. Moving mirror into building 20
30. Mirror on hoisting cables inside chamber 20

Abstract

The modification of the JPL 25-ft space simulator to produce a larger and higher quality beam evolved a 23-ft-diam, single-piece, spherical, 50-ft focal length mirror. The thermal control restraints, as well as the optical specifications, had a major influence on the final configuration selected. The mirror structure was carefully machined after weld-fabricating. Then the structure was electroplated with nickel, contoured and polished, and, finally, aluminized. The great size of the mirror required the development of several new fabricating techniques. The use of these techniques and recommended modifications should be advantageous in the production of future metal mirrors of this type.

Fabrication of the 23-ft Collimating Mirror for the JPL 25-ft Space Simulator

I. Introduction

The 23-ft diam mirror is an optical element of the solar simulator installed in the modified JPL 25-ft space simulator (Ref. 1). The purpose of this mirror is to reflect the light from the optical integrating lens system in a collimated beam so as to simulate rays of the sun.

The performance of the solar simulator is closely tied to the quality of the collimating mirror. The size of the collimated beam is limited by the size of the collimating mirror. Testing and evaluating large spacecraft with complicated shapes can best be accomplished if the quality of simulated solar radiation approaches that of the sun and the beam encloses the entire model. The design and fabrication of this mirror was based on meeting these goals in a reasonable time at minimum cost.

II. Design Criteria

The new solar simulator installed in the 25-ft space simulator was designed to produce an irradiated test volume 15 ft in diameter and 25 ft high. It was determined that the design would incorporate as much flexibility as possible and have provision for expanding the beam size to a full 20-ft diam and/or increasing the radiation level. Further, it was determined that at a nominal irradiance of 130 W/ft^2, the uniformity should not vary more than $\pm 5\%$ in any plane normal to the optical axis or more than $\pm 10\%$ anywhere inside the test volume.

It was also decided that the mirror should not radiate more energy to the test volume than that radiated by the LN_2-cooled walls. It was known that a temperature of $-100°F$ during test would satisfactorily limit the radiation from the mirror and also inhibit contamination of the reflecting surface by condensation on the relatively warm mirror. JPL determined that the temperature of the mirror should be capable of being changed 170°F in 1.5 h so that the equilibrium test conditions could be reached in a reasonable time. Another requirement for the mirror was that it should be capable of being heated to +200°F during the bake-out of the wall shrouds under vacuum, to prevent contamination of the reflecting surface. Temperature-controlled GN_2 was used for heat transfer in the mirror cooling tubes because of operational requirements of maintaining a clean environment in the space simulator in case of failure of the temperature control system.

Finally, because of the difficulty in producing a large number of welded leak-tight joints in the aluminum heat-exchanger tubing (10^{-8} standard cm^3/s He), the number of temperature control cells had to be kept as low as possible.

III. Design Selection

A. Optical Design

The optical design (Ref. 2) of the SS15B system requires a spherical mirror of 1200 ±12-in. radius. The mirror surface has to be highly reflective and of uniform slope over the entire surface.

To meet all requirements for uniformity of irradiance in the test volume, it was necessary to determine anticipated contributions to nonuniformity. The off-axis angle of the solar beam, and the position of the virtual source, with respect to the collimating mirror in the SS15B system, was optimized by selecting the minimum feasible off-axis angle (14 deg) and moving the virtual source 18 in. above the focus of the mirror (Ref. 3). It was determined that these changes would improve the theoretical nonuniformity of the beam, as a result of the spherical aberration effect, from ±2.7 to ±2.3% and would improve the theoretical collimation on the test plane from 1.59 to 1.08 deg.

Data obtained from a precision-scale mockup of the SS15B system showed that the nonuniformity varied linearly with slope (approximately 1:1) for a 2-deg field angle so that a 1.0-min slope deviation was equal to 1.0% nonuniformity. It was arbitrarily decided to allow ±30 s for possible slope deviations of a segmented collimating mirror which would contribute ±0.5% to the nonuniformity. Prior experience with the JPL 10-ft mirror showed that ±30 s would be easily obtained with a one-piece 23-ft mirror.

Prior testing of nickel-plated aluminum samples showed that durable, highly specular surfaces could be obtained by vaporizing aluminum on the sample within a vacuum. The electron beam gun method of heating the aluminum in a crucible 18 ft from the center of the mirror was found to deposit aluminum over the surface of the mirror about 650 Å at the edge to 1200 Å at the center with a total reflectance uniformity of better than ±1.0%.

The mixer lenses in a 19-lens array contribute approximately 1.0% to the total nonuniformity in the test volume with the distribution of energy produced by the Hanovia 20-kW lamp in the JPL elliptical collector assembly.

The total of the aforementioned contributions to nonuniformity is ±4.8%, leaving a remaining ±0.2% to be accounted for by gaps in a segmented mirror or defects, such as blisters or pits in the mirror surface. These nonuniformities were found to be as follows:

Nonuniformities	Tolerances, %
Spherical aberration	±2.3
Slope deviation	±0.5
Reflectivity	±1.0
Mixer distribution	±1.0
Gaps or defects	±0.2

Figures 1 and 2 show curves describing nonuniformities resulting from defects and gaps in the mirror surface. If a tolerance of ±0.2% were to be maintained, then gaps of

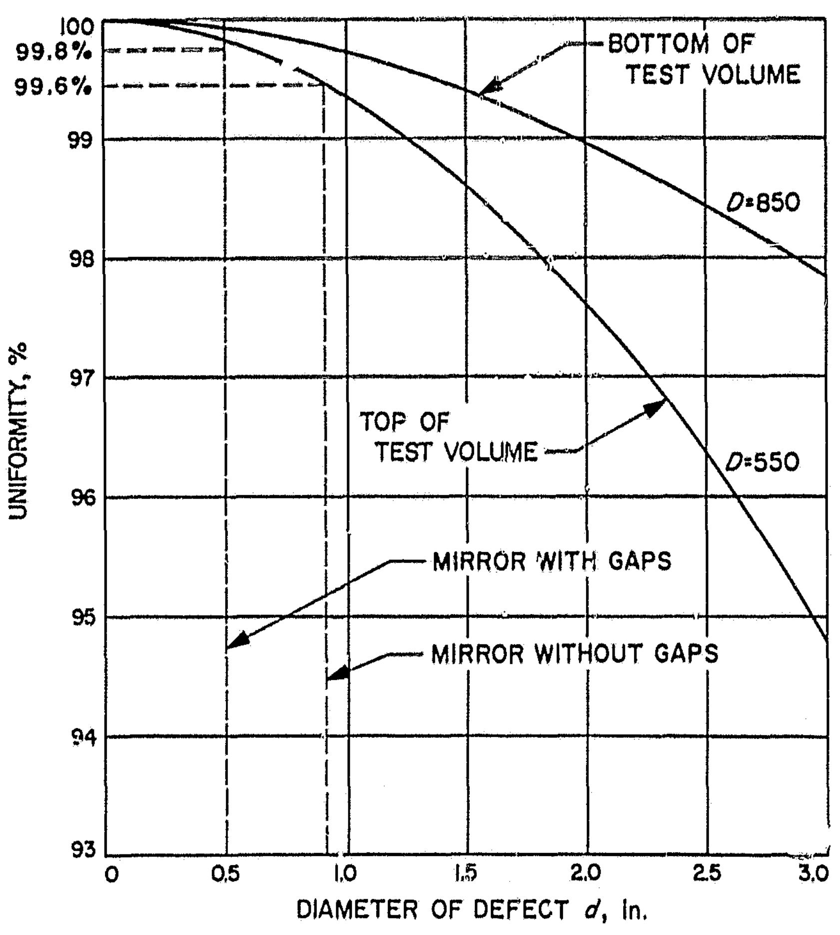

Fig. 1. Uniformity vs diameter of defect for 1-deg half-angle

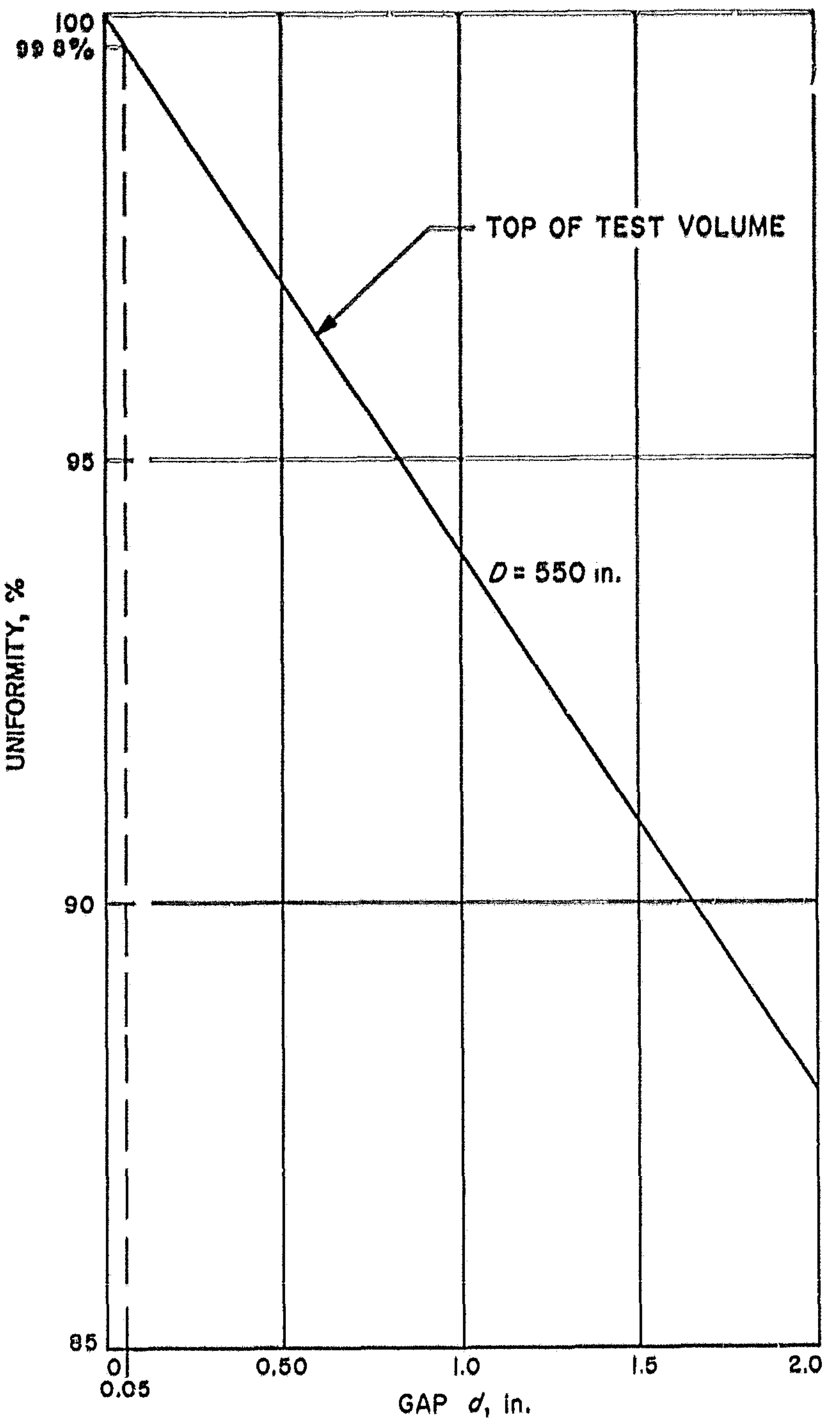

Fig. 2. Uniformity vs gaps for 1-deg half-angle

less than 0.05 in. or round defects of less than 0.5 in. diam had to be maintained over the entire mirror surface. This was believed to be a difficult task to accomplish in making a multi-segmented mirror of such large size. This task also pointed up one of the difficulties of producing a solar simulator that has a highly collimated beam. The 23-ft mirror, therefore, had to be produced by using a one-piece design or a sophisticated design minimizing the structural nonhomogeneities and interconnecting gap clearances.

B. Structural Design

A general study was made of the mirror requirements and how best to meet them from a structural standpoint. The 1200-in. radius of curvature of the mirror gave a rise of the spherical dome of some 8 in. This rise/span ratio was so small that the mirror could have been considered as a flat plate. To make the deflections and thermal deformations from such a structure as uniform as possible, the structure chosen was a 60-deg webbed, geodesic rib pattern supporting a continuous plate (Fig. 3). It was also determined that this pattern would be very efficient from a weight vs rigidity standpoint.

In order to minimize temperature differences in the mirror, using a cooling coil with each mirror rib cell, it was required that a nominal 2-in. section be used. This requirement was based on the concept of each cell consisting of a triangular plate with an inscribed circular cooling coil, using a method suggested by Hickman (Ref. 4). The actual front face thickness specification was finally set at $2\frac{1}{4} \pm \frac{1}{4}$ in. because of the difficulty in weld-fabricating a plate of such large size and maintaining the radius of curvature.

An existing computer program developed by Batchelder and Wada (Ref. 5) was used to study the weight vs rigidity and to complete the structural design. Because the rib pattern, front face thickness, and rib thickness were determined largely from thermal constraints, the rib height parameter was varied, and the resulting deflection, point slope, and mirror weight were calculated. Figure 4 shows the result of this study and the design point selected: a maximum 1-g deflection of 0.019 in. with a total mirror weight of 25,000 lb. The point-slope deviation at this point was 1.0 min maximum from the desired curvature.

The edge support system was selected to support the mirror structure in order to minimize structure distortions and to make the slope deviations as small and uniform as possible. By using a whiffle-tree type of mount, it was possible to support the mirror structure on 12 points around the periphery and, ultimately, to permit final installation in a 3-point, easily adjustable suspension from the top of the simulator chamber. Ball-jointed bearings or pins provided low-friction mobility that would allow the structure to change size, without introducing loads into the chamber or mirror and thereby cause optical misalignment. Stainless-steel and aluminum-bronze turnbuckles were used for low friction adjustment and positioning of the mirror. All materials were selected on the basis of being compatible for a high vacuum-cryogenic environment and were stress-designed for a safety factor of at least 5. A redundant stainless-steel cable support structure is provided which also allows for hoisting the mirror into position inside the chamber.

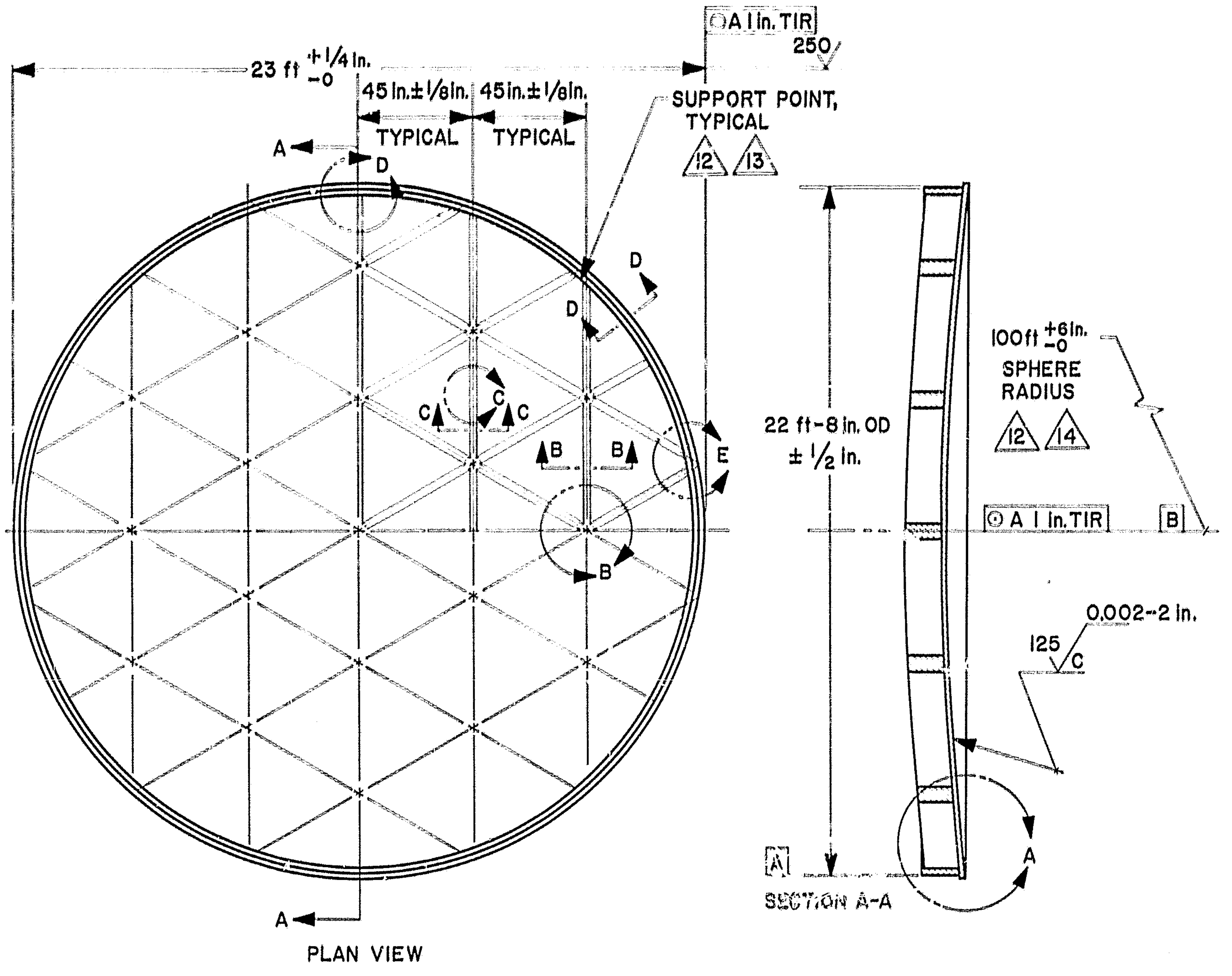

Fig. 3. The 60-deg webbed, geodesic rib structure supporting continuous plate

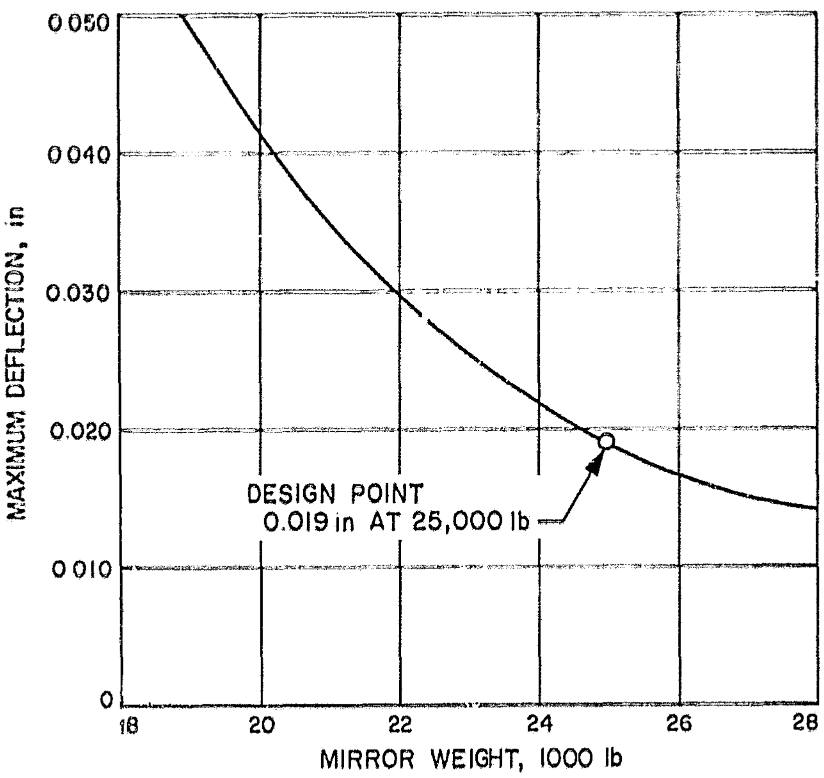

Fig. 4. Results of deflection vs weight study

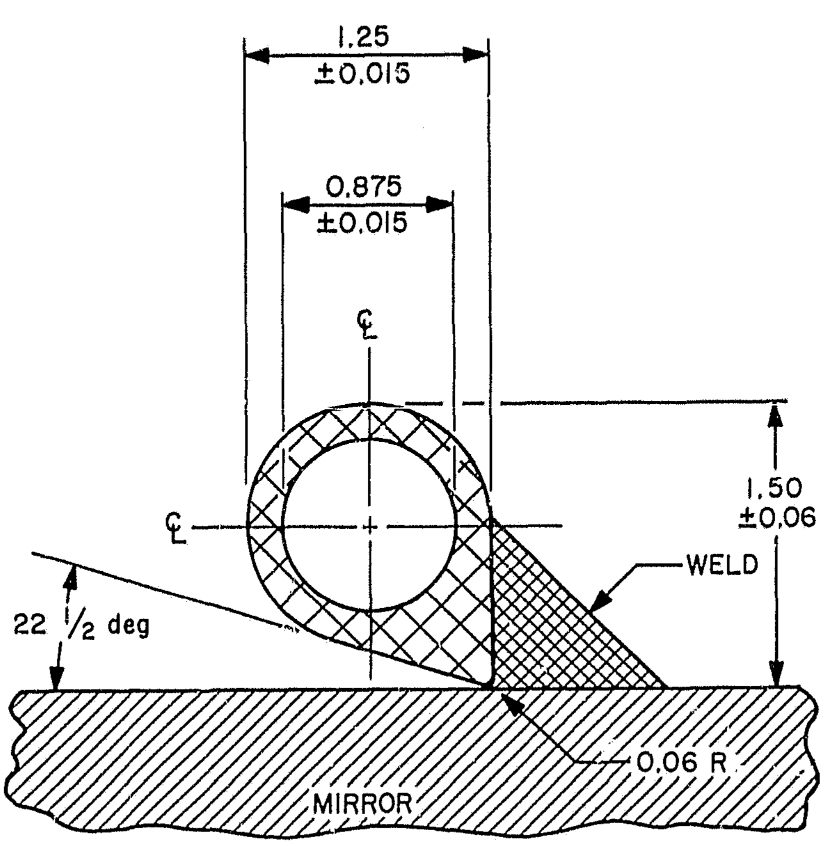

Fig. 5. Gas heat-exchange tube

C. Thermal Design

Maintaining the mirror at $-100°F$, while being irradiated by the solar beam, is a relatively easy task compared to the restraint of cooling the mirror from $+70°F$ to $-100°F$ in 1.5 h. The heat removed during steady-state operation should not be greater than

$$q_R = \phi\alpha A = \frac{275}{0.85}\,\frac{\mathrm{W}}{\mathrm{ft}^2} \cdot (0.1)\,(177)\,\mathrm{ft}^2\,(0.0569)\,\frac{\mathrm{Btu}}{\mathrm{min/W}}$$

$$q_R = 325\,\frac{\mathrm{Btu}}{\mathrm{min}}$$

whereas, the heat-removal rate q_R to cool the mirror is about

$$q_R = mc\Delta T = 25{,}000\ \mathrm{lb}\,(0.2)\,\frac{\mathrm{Btu}}{\mathrm{lb\text{-}°F}}\,(170)\,°\mathrm{F}\left(\frac{1}{90}\right)\mathrm{min}$$

Finally,

$$q_R = 9450\,\frac{\mathrm{Btu}}{\mathrm{min}}$$

The size of the temperature control system is based on this higher rate, and the blower should be sized to move this amount of gas (CFM). Thus,

$$CFM = \frac{9450\,\dfrac{\mathrm{Btu}}{\mathrm{min}}}{(0.356)\,\dfrac{\mathrm{lb}}{\mathrm{ft}^3}\,(0.24)\,\dfrac{\mathrm{Btu}}{\mathrm{lb\text{-}°F}}\,(75)\,°\mathrm{F}} = 1480\,\frac{\mathrm{ft}^3}{\mathrm{min}}$$

The blower design selected for this application is suitable for a case pressure of 100 psig with a temperature range of $-300°F$ to $+200°F$. The capacity is 1500 ft^3/min at a 4.0-psig head differential allowing approximately 2 psi ΔP for the mirror and a 2-psi drop for the rest of the plumbing.

The mirror temperature control system was chosen to be a recirculating GN_2 system because of the operational requirement of limiting damage to test components in the event of a line failure inside the space simulator.

Special gas heat-exchange tubes were fabricated to allow easy welding to the rear of the mirror face and to provide a large heat path area through a minimum distance (Fig. 5) of the weld joint.

The structural layout of the mirror ribs included 54 individual cells on the rear surface. Each cell is temperature-controlled by a single gas tube in order to facilitate the welding operations and minimize possible leaks at the manifold-tube connections. The gas tubes were mounted in each cell so that they would minimize the temperature gradients in each cell during transient cooldown and steady-state operational heat loads on the front face of the mirror.

A special test was run on a full-scale instrumented mirror cell to observe temperatures vs time for various cooldown rates. This test was conducted to check the thermal design and to predict performance of the finished mirror. The cell was mounted in a vacuum chamber and irradiated with tungsten lamps. Because this model's front surface had not been polished and aluminized, the front surface was painted flat black and the irradiance was scaled down to compensate for the absorptivity change and to provide an equivalent heat load. The sides of the model were wrapped with 10 layers of aluminized Mylar insulation so as to provide a thermal barrier (Fig. 6).

The first configuration tested involved a circular cooling ring because it was thought that the fabrication of such a ring would be easier and would not cause appreciable gradients in the front face temperatures. The gradients in the front face were greater than anticipated, however, and the design was changed to a triangular configuration to reduce the gradient.

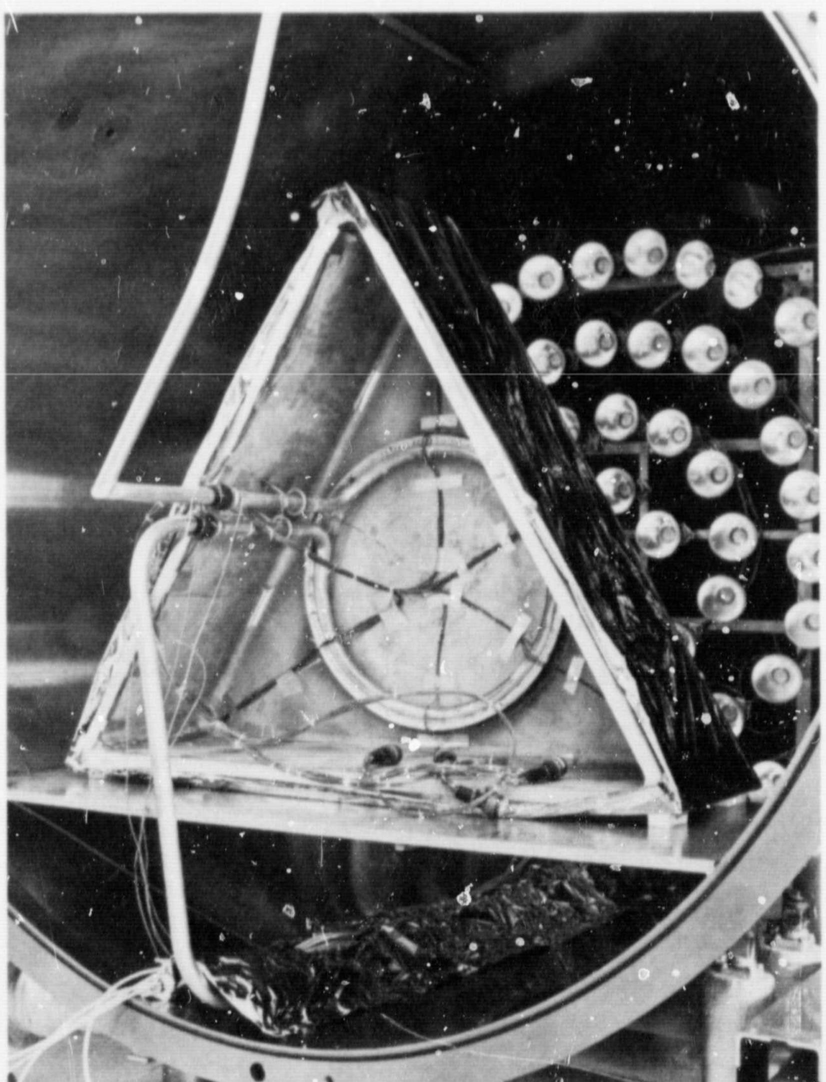

Fig. 6. Aluminized Mylar insulation

Figure 7 shows the temperature gradient between the mirror front face and the extreme back of the rib structure vs the temperature rate change for the modified test model and the finished mirror. Note that the steady-state temperature gradients were zero for lights-off and 2°F and 6°F for earth and Venus intensities, respectively.

The size of the heat-exchange tubes was determined by equating the heat removed from the mirror to the heat transferred through the gas-tube interface, which can be expressed as

$$q \text{ removed} = q \text{ transferred}$$

$$mc\Delta T_{\text{cell}} = HA\Delta T$$

where

$$H = \frac{k}{D} 0.023\, (N_{Re})^{0.8} (N_{Pr})^{.03}$$

$$T_{\mathrm{MGN_2}} = -150°\mathrm{F}$$

$$P_{\mathrm{GN_2}} = 52 \text{ psia}$$

$$N_{Re} = \frac{\rho Q D}{\mu A}$$

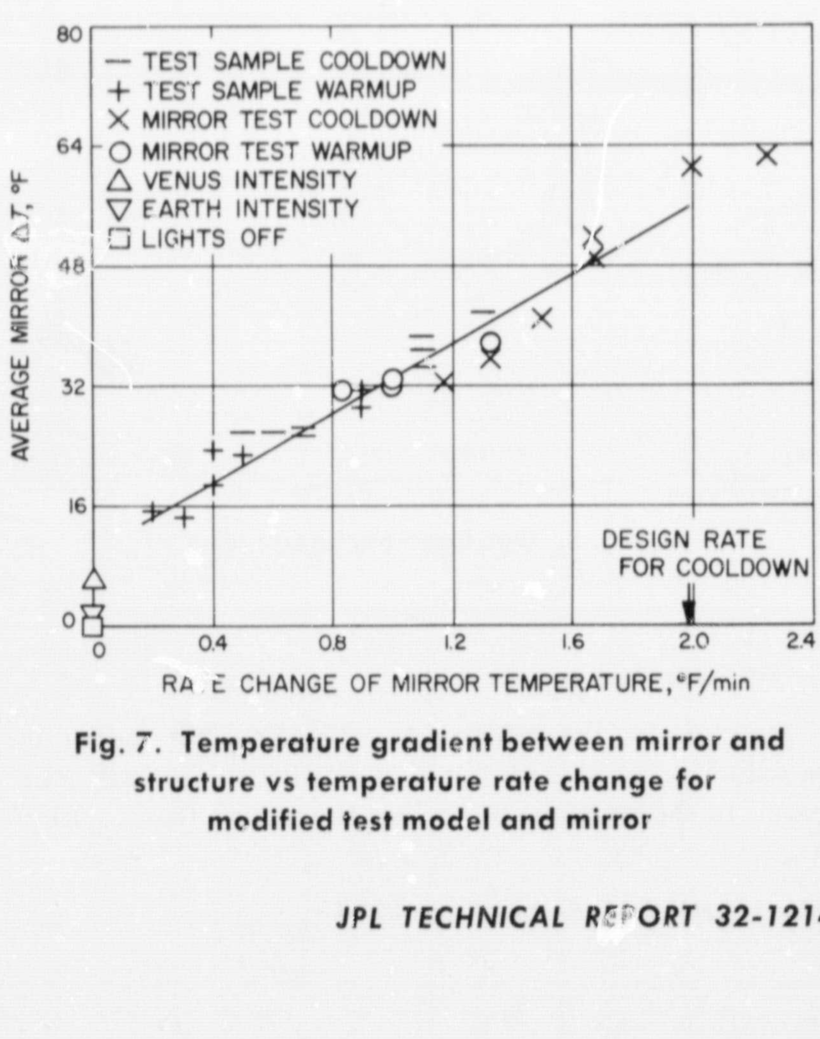

Fig. 7. Temperature gradient between mirror and structure vs temperature rate change for modified test model and mirror

Substituting the proper values gives

$$Q = D\left(\frac{122}{t}\right)^{1.25} \quad (1)$$

where

Q in ft³/min

D in ft

t in h

The pressure drop in the tubes for various flow rates and tube diameters is shown in Table 1 and can be calculated by using the Darcy–Weisbach equation:

$$\Delta P = \frac{f}{D} L\rho \frac{V^2}{2g}$$

where

f is an average of 0.013 for the velocities being studied

$$T = -150°\mathrm{F}$$

$$P = 52\,\mathrm{psia}$$

Substituting $V^2 = \dfrac{16Q^2}{\pi^2 D^4}$, the equation can be rewritten

$$Q = \left(\frac{\pi^2 g \Delta P}{8fL\rho}\right)^{0.5} D^{2.5} \quad (2)$$

where

Q in ft³/s

ΔP in lb/ft²

D in ft

Table 1. Pressure drops in mirror temperature control system

Item No.	Piping	Pressure drop ΔP, psi
1	6-in. to 1.61-in. contraction	0.0175
2	70-in. length of 1.61-in. ϕ and two 90-deg bends	0.0363
3	1.61-in. to 1.278-in. contraction	0.0115
4	17-in. length of 1.278 and one 90-deg bend	0.0324
5	0.875-in. extrusion (heat-exchange tube)	1.010
6	Same as item 4	0.0324
7	1.278-in. to 1.61-in. enlargement	0.0136
8	Same as item 2	0.0363
9	1.610-in. to 6.0-in. enlargement	0.0338
10	6-in. manifolds (inlet and outlet)	0.0468
Total $= \sum_{i=1}^{10} \Delta P_i$		2.247

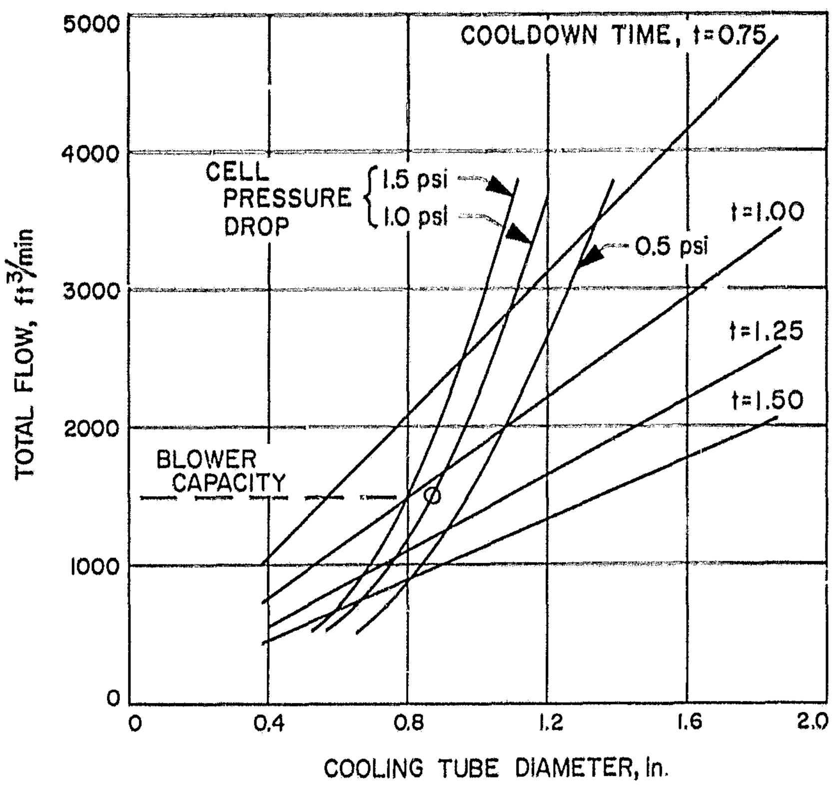

Fig. 8. Total flow vs tube diameter

Figure 8 is obtained by plotting Eqs. (1) and (2). The selected design point is at a tube diameter of 0.875 in. and a flow rate of 1500 ft³/min. This point yields a pressure drop of 1.0 psi and a cooldown time of less than 1.5 h for maximum rates.

IV. Fabrication Techniques

A. Fabricating the Weldment

The following four methods of fabrication were investigated:

(1) One-piece mirror (weldment or casting)

(2) One-piece mirror made from six or seven prefabricated pieces.

(3) Seven-piece mirror bolted together to form an assembly. (The mirror to be machined, ground, and polished as an assembly.) It may be transported, plated, or aluminized as individual pieces or as an assembly.

(4) Same as (3), except that the pieces are ground and polished separately.

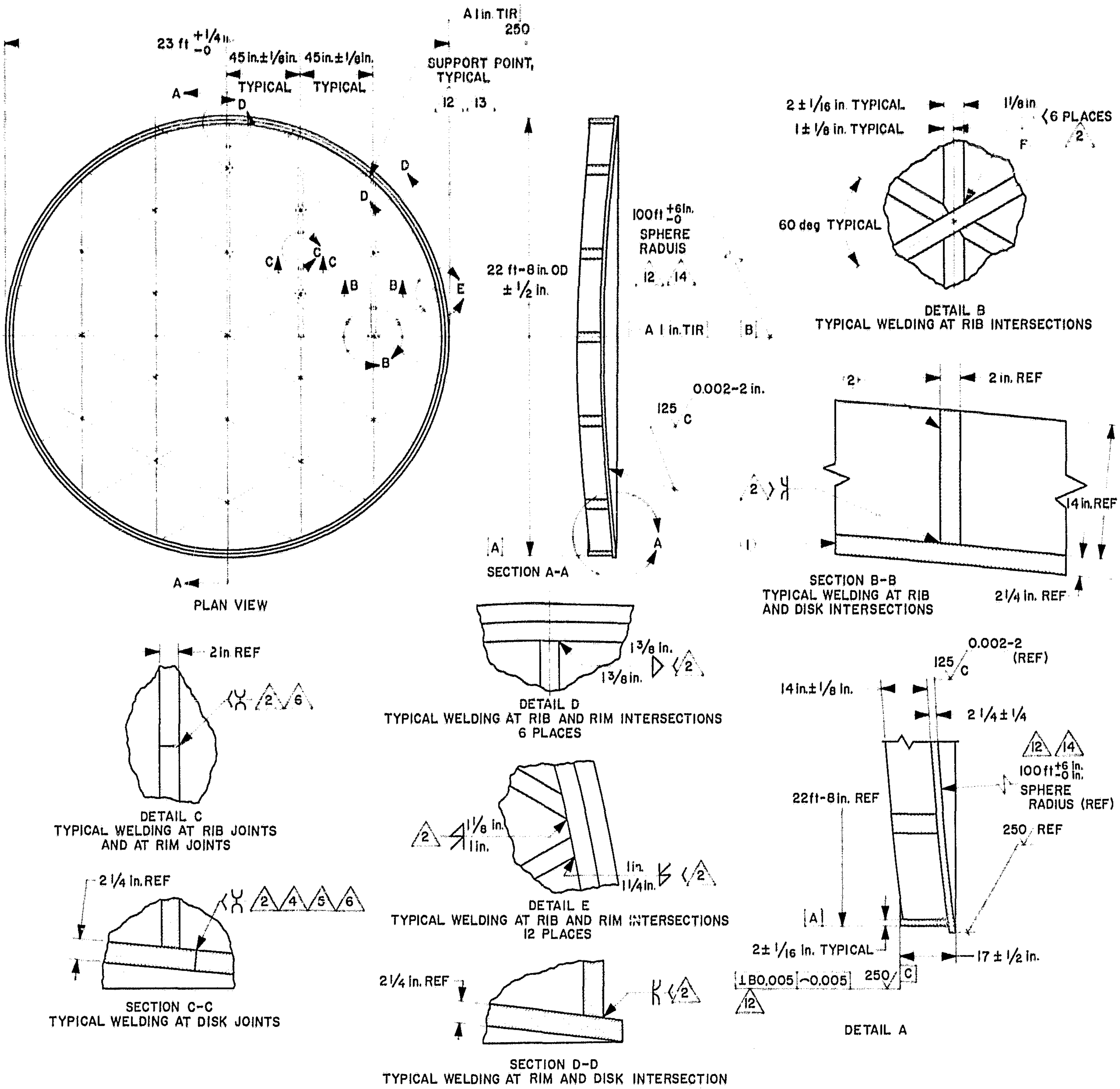

Fig. 9. Fabrication specifications

18. Any rib member may be a through member.

17. All double J weld grooves between ribs and disk should have a minimum throat of ⅝ in. to allow proper access for MIG.

16. All dimensions are to be referenced to 68°F.

15. Drilled holes for support and handling to be added.

14. Surface contour must be held to within 0.010 in. relative to a basic spherical radius within the −0-to +6 in.-tolerance range specified.

13. Each of the 12 support points must support one-half of the weight of the mirror ±100 lb. Load cells and instruments will be provided by JPL.

12. When machining 100 ft −0 in.-radius, support assembly on surface -C- at intersection of ribs and rim — 12 places only. 13 F

11. After all welding and before final machining assembly, stress relieve for 10 h (minimum) at 440°F ±10°F, furnace cool-stress relief must be certified. Or, the mirror may be stress relieved at 650°F ±15°F for 1 h, furnace cool and certify. Support the mirror on the welding fixture during stress relief. The mirror must be free to expand independently of the welding.

10. Weldment inspection and approval by JPL cognizant engineer is required before stress relief.

9. Machine front of rib structure and back of disk before welding the rib structure to the disk or the vendor may machine each rib to a matching radius and weld separately. The gap between the rib and the dish must not exceed 3/32 in.

8. Preheat and interpass temperature of up to 200°F may be used, if necessary.

7. Cracked or broken welds, or welds of otherwise poor quality, shall be removed by chipping or grinding, and shall not be welded over into the final weld or member. Cold starts, weld cracks or crater cracks, or undercuts shall be chipped out and repaired. Unfilled craters shall be filled. Dye check to be used to determine holes or cracks in weldment.

6. Double welded U-joints which have a root opening shall be back-chipped or ground on the under side.

5. The U-joint on the front surface of the dish face must be mechanically cleaned before welding machined surfaces, clean with acetone, and then clean with rotating SST wire brush (5000 fpm surface speed) — welding must be done within 6 h after cleaning.

4. Weld for minimum porosity on front face of disk-automatic welding. Porosity in disk fabrication seams to be no greater than Assorted drawing, Section 8, ASME Pressure Vessel Code, for 4-in. weld, Winter 64 Addendum. All holes discovered on disk face after final machining greater than 1/16-in. diam will be filled after consulting JPL cognizant engineer.

3. Use 5356 Al Aly filler wire for all welding — 1/16 to 3/32 diam.

2. All welding is for heat transfer as well as structural and must be 100% continuous welding except for the area between the ribs and the front face at the intersections of the ribs.

1. All welders must be qualified on ASME Section IX performance or on operator qualification tests with the welding process to be used.

Fig. 9 (contd)

Fabrication method 1 could not be used for a casting process because no company could be found willing to risk a casting this size on a fixed-price contract. Method 3 was dropped from consideration because of the mirror gap constraint and also the anticipated problems in joining the assemblies. Method 4 was found to have no significant advantage over 3 because the cost of building a grinding and polishing machine for method 3 was about the same as the added cost of grinding and polishing seven odd-shaped segments individually. Grinding and polishing seven segments individually would have produced seven different radii of curvature, which would only add to the nonuniformities of the system.

Fabrication method 2, therefore, appeared to be the most logical choice for making the 23-ft collimator by welding together six pie-shaped pieces. After going through the procurement cycle for the six castings, it was found that the low bidder could not do the work because of contractual problems. At this point, the cost and delivery of a one-piece weldment became superior to that of the next lowest bidder on method 2.

Fabrication of wrought aluminum plate also provided several advantages over that of joining castings. The welds on wrought plate are not as porous as that of a welded casting, which is better for the nickel plating. Also, the high silicon content in the aluminum casting (355A or 356A) causes considerable problems with the Kanigen nickel-plating process.

The fabrication specifications shown in Fig. 9 were taken from JPL drawing 6-9374334. The metal chosen for the front face and rib structure was 5086-H112 aluminum plate (special mill run because of its thickness) for many reasons: (1) good strength in the fully annealed condition, (2) resistance to corrosion, (3) excellent weldability, (4) good long-term dimensional stability, and (5) compatibility with anticipated nickel-plating techniques. One of the disadvantages of the 5086 alloy is that the thermal conductivity at cryogenic temperatures is lower than some of the other alloys.

The fabricating contractor bolted six 3-in. preshaped plates to a welding fixture (Fig. 10). The welding fixture was machined to a 100-ft radius. After fitting and bolting the plates to the fixture, the plates were joined by welding with a manual inert gas (M.I.G.) machine through the fixture back (Fig. 11). After welding, the backs of the plates were machined to a 100-ft radius on a 40-ft vertical boring mill (Fig. 12).

The ribs were machined as necessary to fit the pattern on top of the machined plate section. Five ribs were run

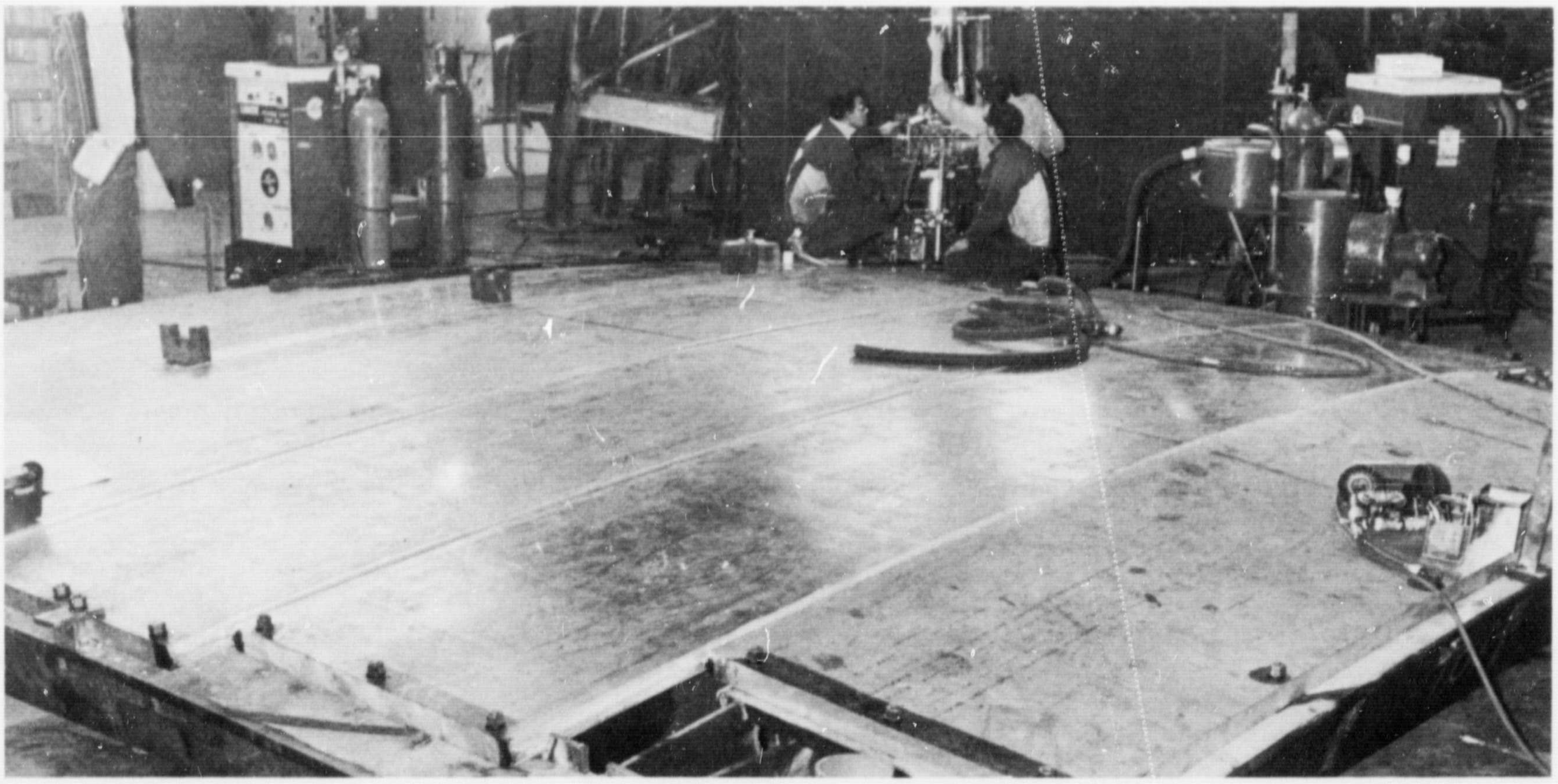

Fig. 10. Bolting preshaped plates to welding fixture

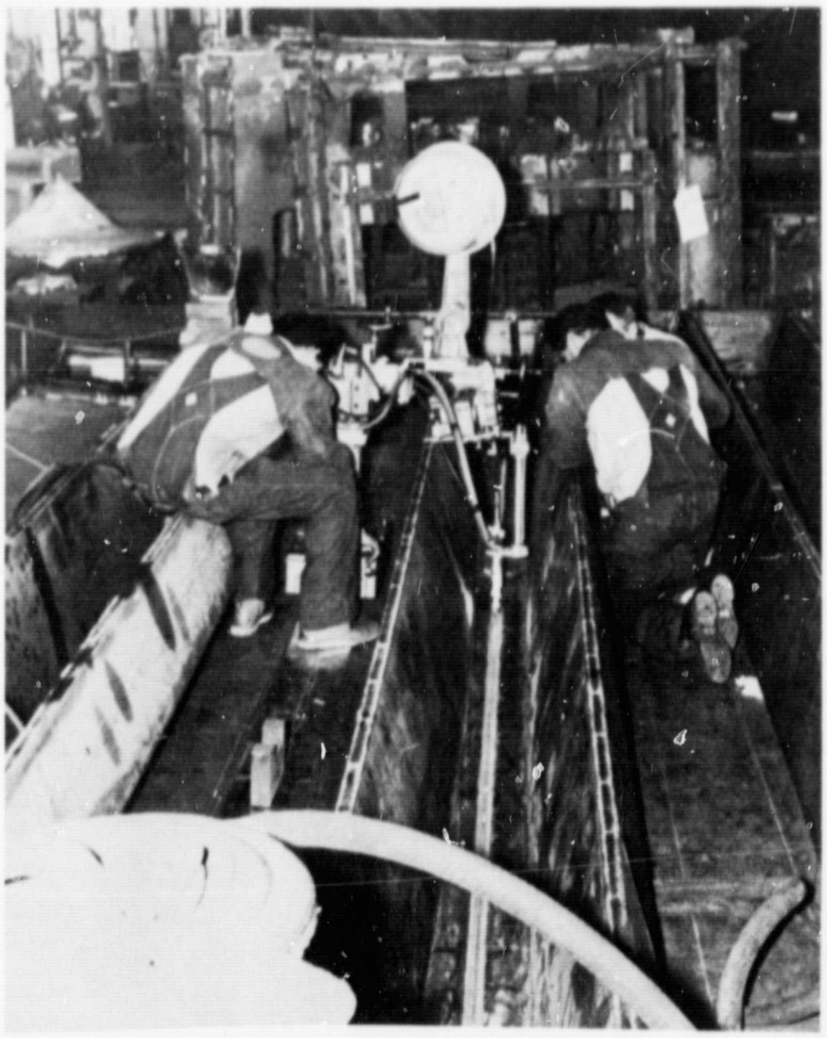

Fig. 11. Welding front face through surface back

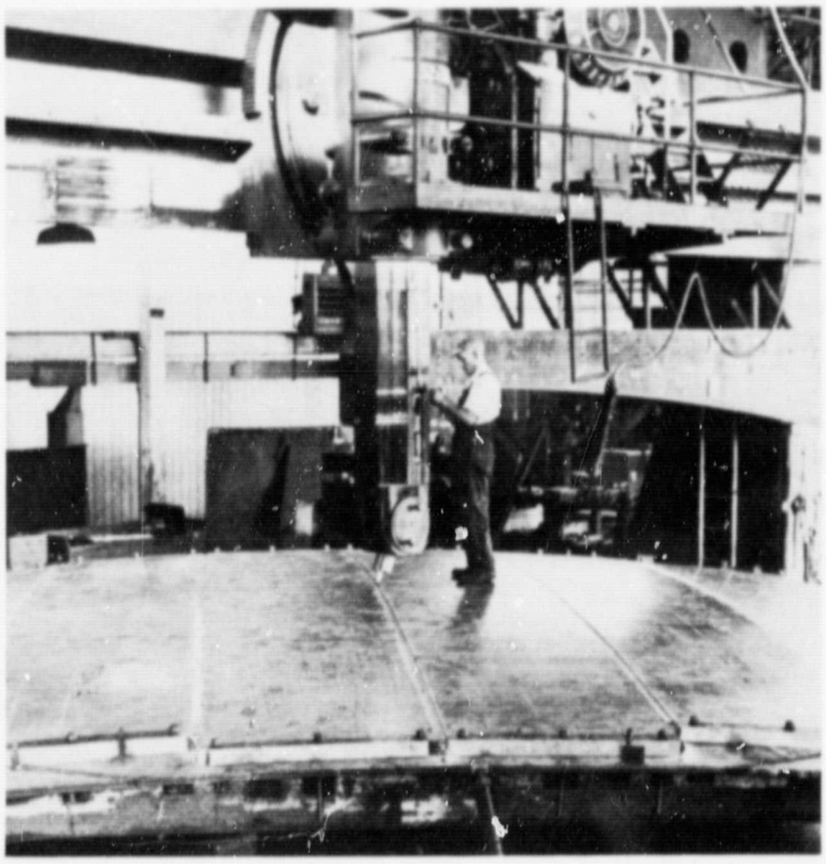

Fig. 12. Machining by 40-ft vertical boring mill

completely across the mirror back and the others were cut to fit. The outer ring was fabricated from three pieces rolled to a 11-ft, 2-in. radius. Welding of the ribs to the back of the front face plates is shown in Fig. 13.

Prefabricated cooling coils were welded inside each rib cell, as shown in Fig. 14, and the excess plate material was trimmed off the OD of the mirror, and the top of the outer ring was trimmed off.

Inspection of the mirror weldment, after release from the welding fixture, revealed that the finished radius of curvature was 112 ft instead of the specified 100-ft radius. The contour mapping of the mirror surface, after stress relief, revealed that the radius was longer in a direction 90 deg to the weld seams. It is believed that the distortion of the mirror, after removal from the welding fixture, could have been prevented by using other fabricating techniques. To prevent the unequal distortion of the weldment, the welding fixture could have been made equally stiff in all directions, rather than in the direction of the weld seams only. Another factor contributing to the distortion was that the rib structure was not completely fabricated as an assembly and machined to a close radius fit before welding to the disk, but instead was cut, fitted, and welded to the disk in small pieces.

There was considerable concern at this point on whether the weldment could be machined to the correct 100-ft radius without regard to the disk thickness specification of $2\frac{1}{4} \pm \frac{1}{4}$ in. because of cutting through to some voids. Although the drawing specification had specified 100% welds on the disk seams, it was learned that the fabricator had used double-J weld seams with ⅝-in. butt joints. It was doubtful whether 100% penetration could have been obtained with the current and size of welding rod used for this operation.

To restore the weldment to the correct dimensions, it was decided to attempt accelerated creep-sagging the weldment in a stressed condition at elevated temperatures. The mirror was placed in the same oven which had been used earlier for the stress relief after welding (Fig. 15). This temporary, electric oven was constructed of an 8-in. reinforced concrete slab with an additional 6-in. circular slab, the size of the mirror, placed on top of the bottom slab. A layer of standard firebrick was placed upon the top of the 6-in. slab and a pattern of nichrome heating elements was arranged uniformly atop the firebrick. The

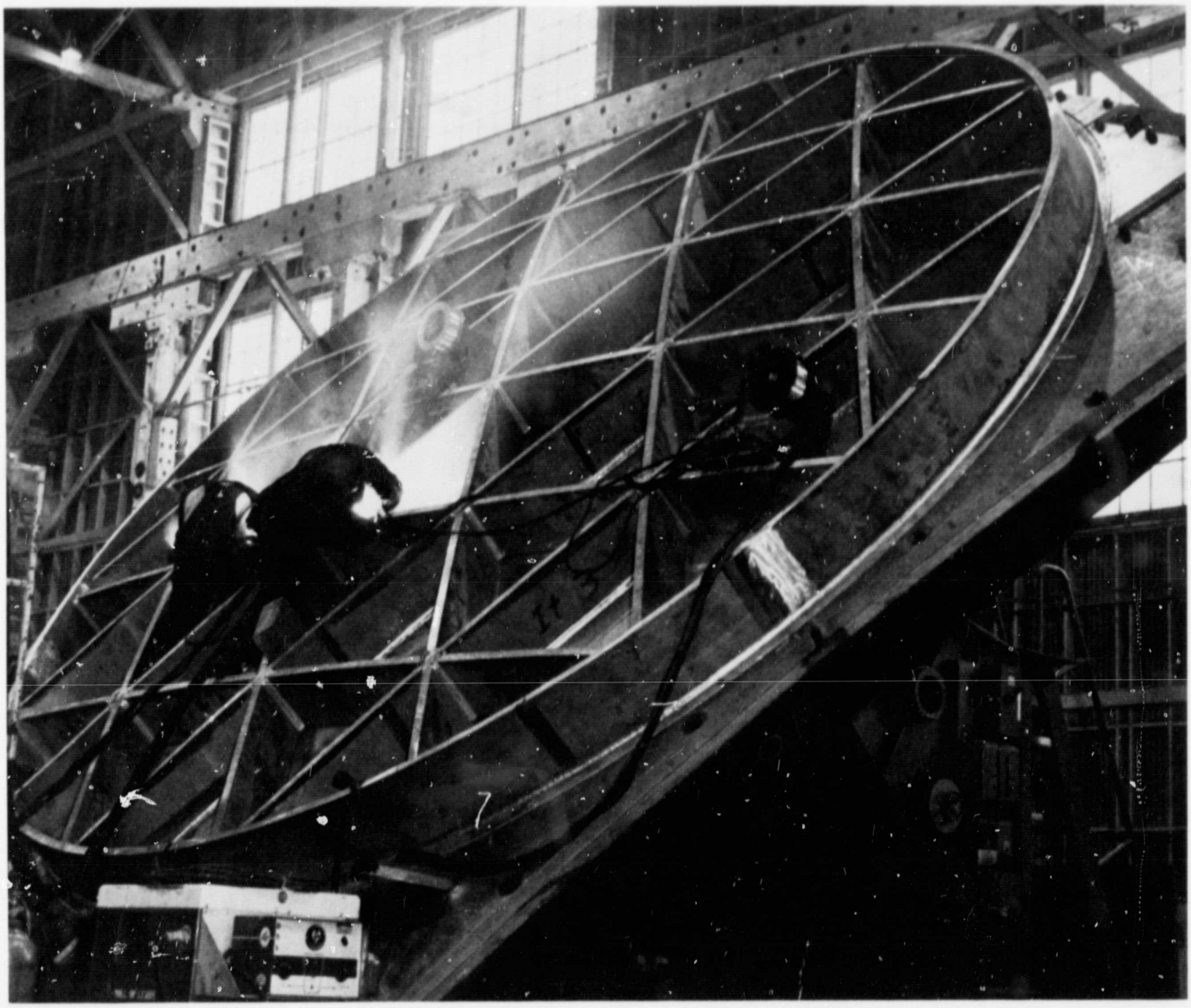

Fig. 13. Welding ribs to back of front face plates

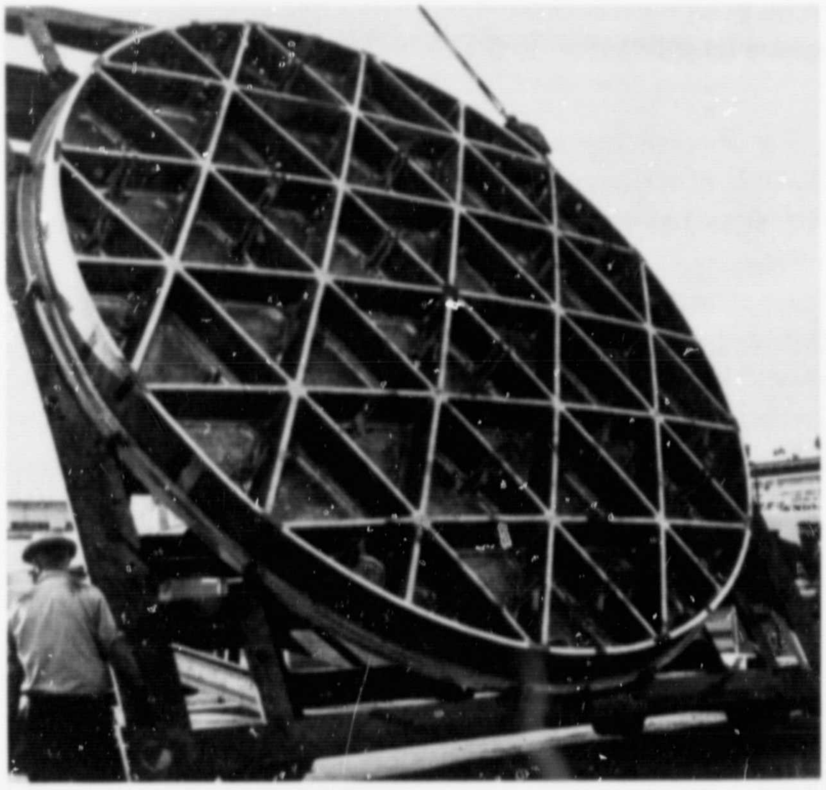

Fig. 14. Cooling coils welded inside each rib cell

mirror was supported on 12 outer supports and had seven inner stops arranged to give uniform support when the mirror sagged to 0.75 in. at the center (Fig. 16). The sides of insulating block and the thermal blanket top were built up around the mirror.

The center 10-ft diam of the mirror was loaded with 16 tons of dry sand (in sandbags) to stress the weldment in such a manner as to sag the center area (Fig. 17). Figure 18 shows the temperature-creep curves that were obtained from the aluminum manufacturer's laboratory

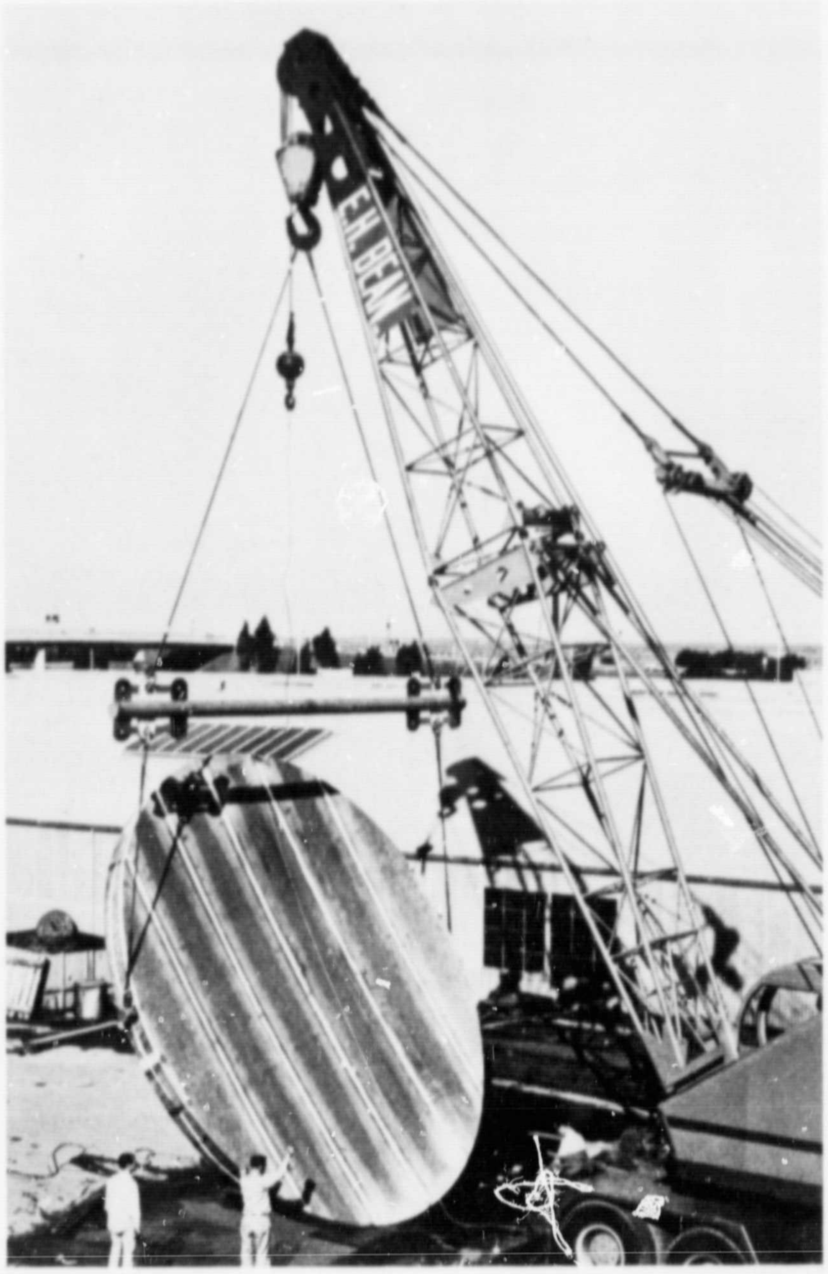

Fig. 15. Unloading mirror for creep-sagging weldment

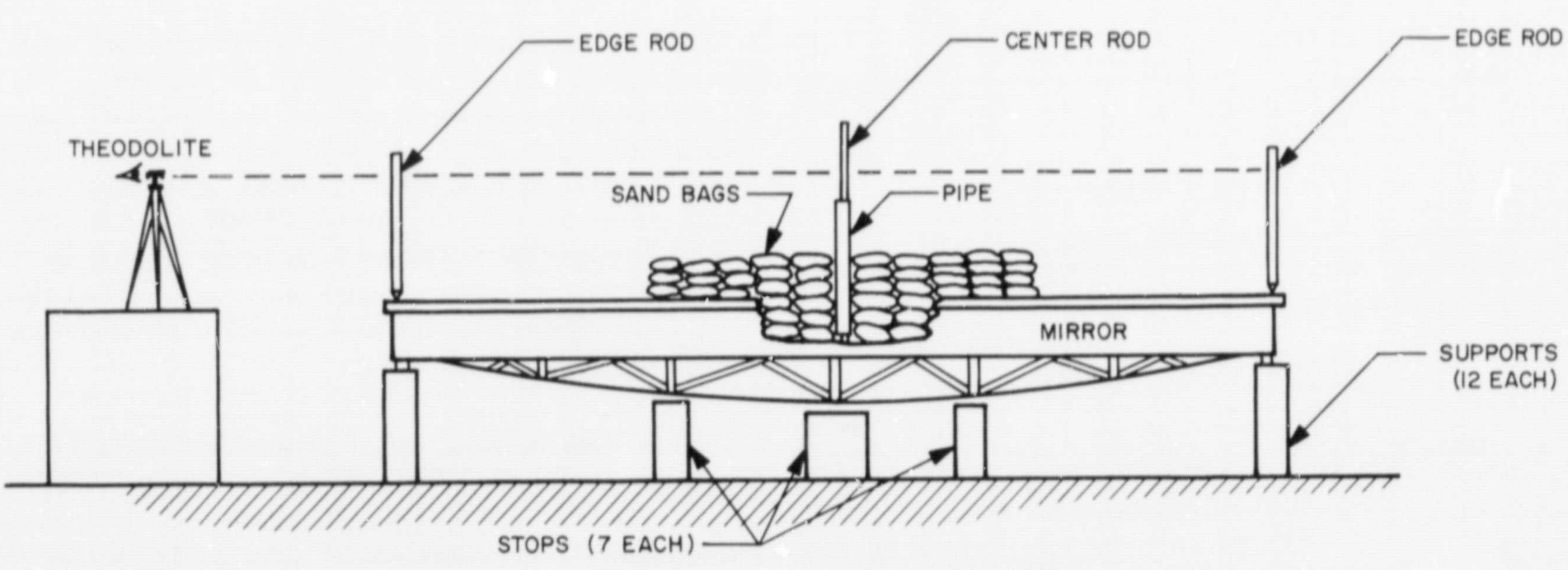

Fig. 16. Mirror loading scheme (insulation not shown)

Fig. 17. Sandbags used to stress center of mirror

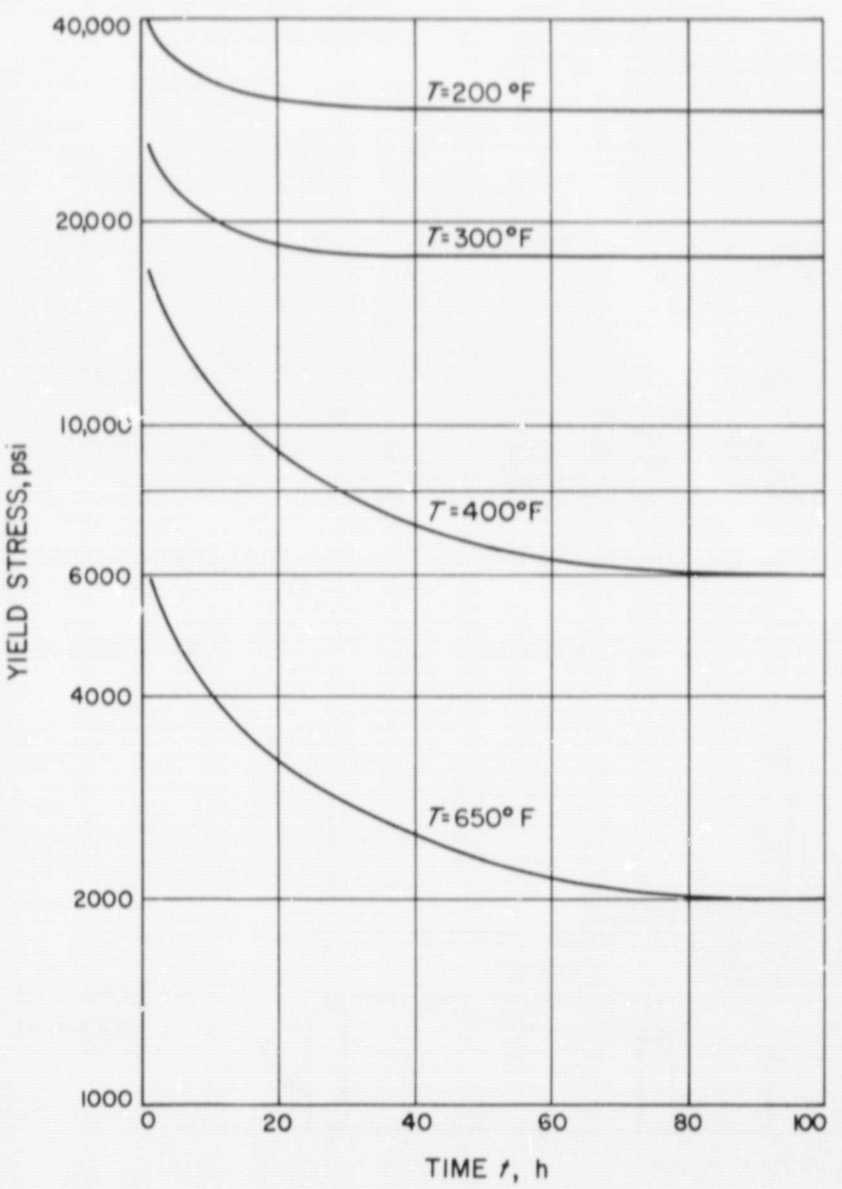

Fig. 18. Temperature-creep curves (10–12%) used for stress operations

to be used for this operation.[2] The mirror temperature was raised to 650°F for 30 h to obtain the 0.75-in. center sag.

To observe the sagging process, a hole was placed in the side of the oven to check when the weldment contacted the stop blocks. Also, a pipe was placed on the front surface of the mirror through the sandbags. A rod with a scale attached was pushed through this pipe and contacted the center of the front surface of the mirror without being restricted by the sandbags. The sagging was observed by referencing the inner rod height to rod heights at the outer edges with a theodolite, as shown in Fig. 16.

The movement of the concrete slab during the heating was so pronounced that observation of the weldment to stop clearance was unreliable. The only reasonable measurements were made by using the theodolite, but these were hampered by the changing heights of the rods during the 30-h period. When the observed difference in rod heights had reached 0.75 in., the heat was turned off and the weldment was furnace-cooled. The sand and the oven were removed after the weldment had cooled to ambient temperatures.

Complete mapping of the front surface disclosed that the mirror had sagged 0.65 in. in the center and that the curvature was closer to the ideal 100-ft radius. Whereas the machining of the mirror weldment prior to sagging would have produced a front face thickness of 2.25 ± 1.0 in., the weldment, after sagging, could be carefully machined to the desired tolerance without the risk of cutting through to a butt joint void.

B. Initial Figuring of Mirror

The final machining was accomplished with the weldment supported at 12 points around the periphery. The support points consisted of a load-washer-and-jack combination to ensure that each point supported 1/12 of the mirror weight, that is, *mirror weight* (30,000 lb) ÷ 12, which meant that each support bore 2500 ($\pm$100) lb. This setup prevented the weldment from being dogged down and machined irregularly, which may have caused the weldment to spring back out of shape when released from the vertical mill.

On the final cut, two events degraded the surface finish. The cutting tool broke after cutting the first 8 in. from the

[2]From telephone conversations with M. Tilley and Dr. Demony of the Kaiser Aluminum and Chemical Corp. Research Laboratory, Seattle, Washington.

edge, and a new tool was installed and set up. This setup produced a slight, but noticeable, step in the mirror surface. This accident also produced a rough area about 0.010 in. deep and 0.5 in. wide for one revolution. Near the center of the weldment, the tool follower on the contour cam ran out of travel and required an additional tool setup. Again, the new setup produced a small (0.002–0.003 in.) step in the mirror contour.

It was believed, then, that these tool marks could be ground out rapidly by the optical contractor, but this was not to be the case. Also, the surface finish and steps in the contour caused great difficulty in measuring the radius of curvature during the final inspection. Figure 19 shows a portion of the inspection procedure used to accept the mirror weldment after final machining. The mirror was undogged from the turntable of the vertical mill and re-checked for load equalization. The measurement of the radius of curvature was conducted by using a large trammel, precision sighting rods, and theodolite. The weldment was considered to have met all of the drawing specifications and was ready for transportation to the optical contractor for grinding the initial shape into the front face.

There was no machine available to grind and polish the 23-ft mirror because it was the largest mirror of its kind built up to this time. A special machine, therefore, was constructed to accomplish this operation. The mirror was mounted on the machine by a 12-point suspension whiffle-tree arrangement so that it was uniformly loaded during the grind and polish operations (Fig. 20).

The machine had several features built-in that were necessary for the plating operation. The rotation speed of the table could be raised up to 5 rev/min in order to permit the plating solutions to be spread over the inside of the concave surface. In addition, the machine and its support structure were designed to carry the weight of the mirror, plus the weight of the plating solution, and to rotate the mirror during plating.

Fig. 19. Inspection after final machining

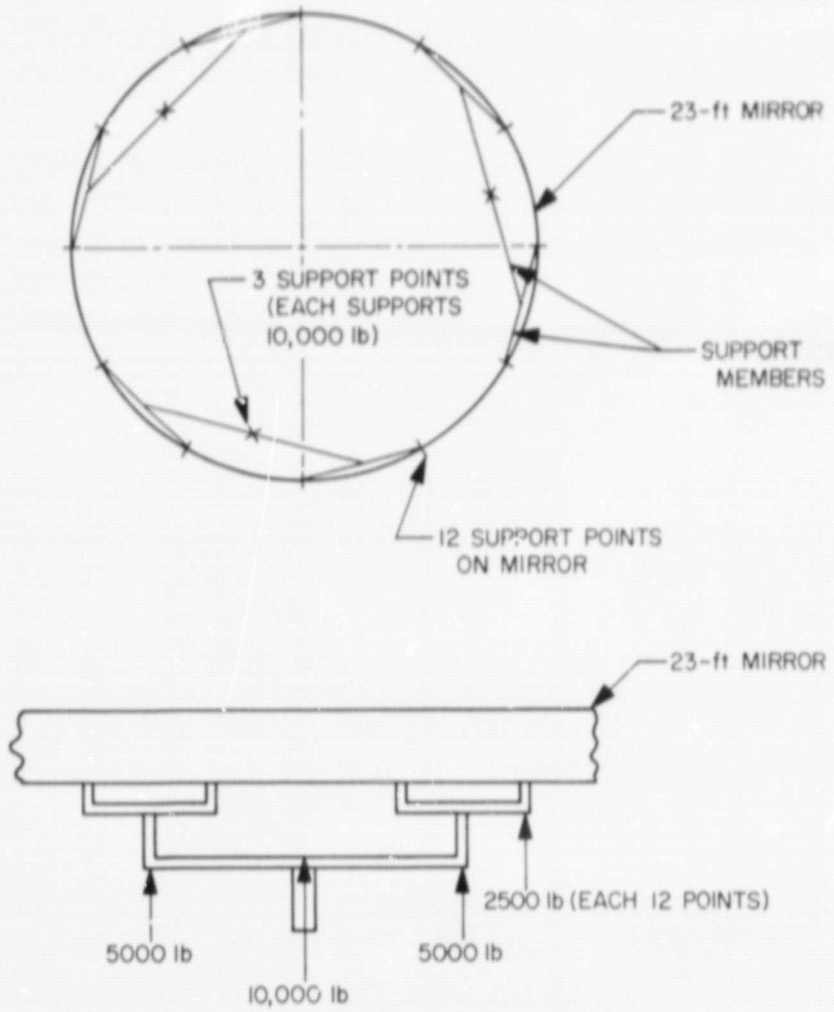

Fig. 20. Grind and polish machine suspension

The first operation was to figure the mirror front face with a 12-ft ring grinder, as shown in Fig. 21. Successively smaller grit sizes were used until the surface was prepared for plating. During this operation it was observed that a better contour and surface finish on the machined weldment would have speeded up the rough grind figuring process.

When the surface was uniformly spherical and of the correct radius of curvature, the mirror surface was inspected and a thorough contour mapping was conducted for use later in checking the plating thickness and uniformity.

C. Plating the Mirror

The nickel-plating operation is described in detail in a JPL Technical Report (Ref. 6).

In general, the mirror blank was electroplated on the mirror grind and polish machine, using the mirror, itself, as the tank and cathode. Nickel anodes were suspended into the solution above the mirror face. The mirror rotation speed and anode positioning ensured equal current density and fairly good uniformity of thickness during plating.

Before attempting to plate the mirror, two studies were made. First, two 12-in. aluminum disks were electroplated

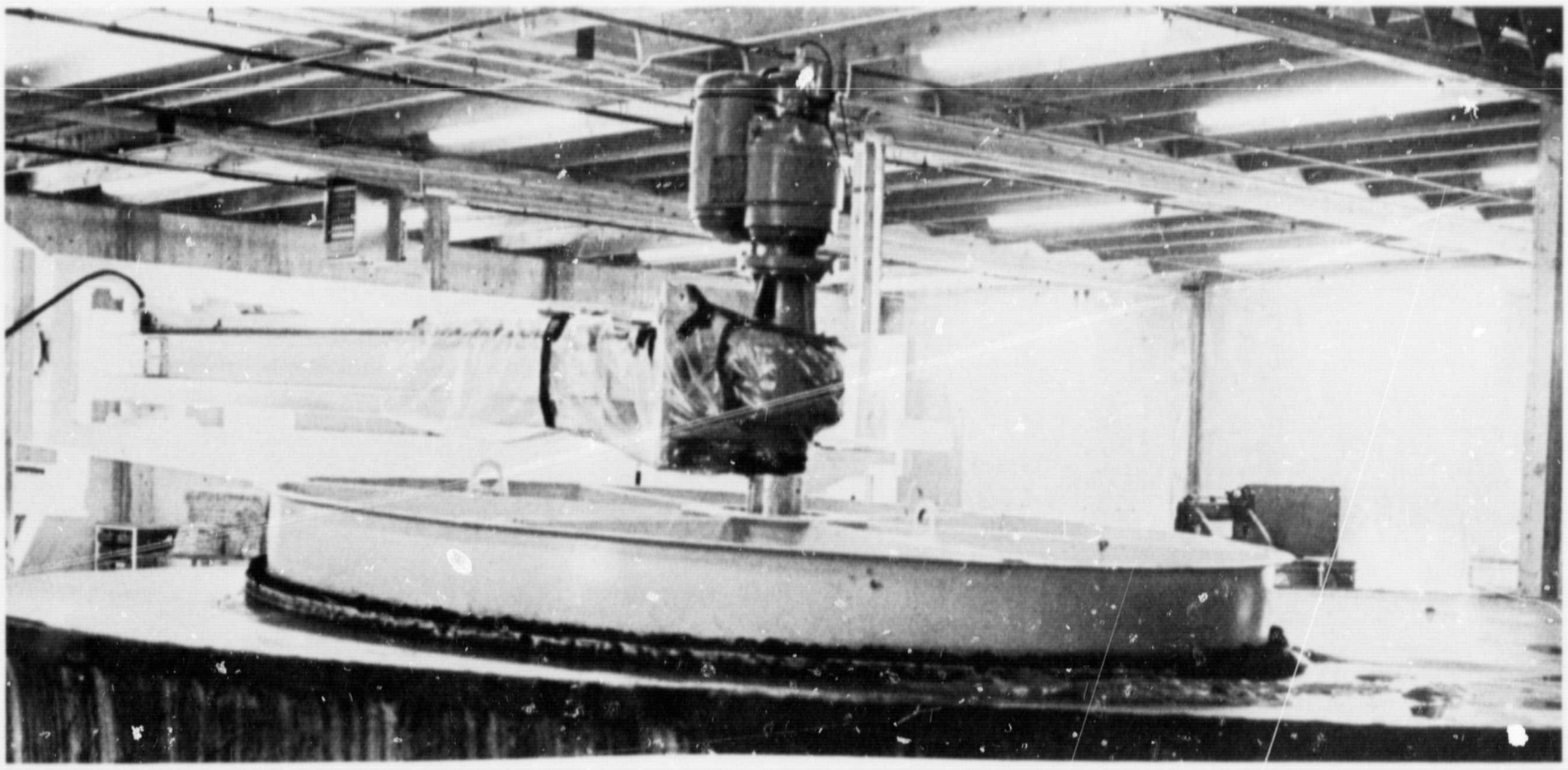

Fig. 21. Figuring mirror with 12-ft ring grinder

with solutions thought to yield the most promising grind and polish characteristics. These samples were plated and then submitted to the optical contractor for use in experimenting with various figuring techniques. The results of this study made it possible to determine the type of nickel-plating solution and grinding and polishing techniques to use.

The second study was made by plating a 4-ft aluminum disk contoured and machined to the same specifications as the 23-ft mirror. In this study, several surface defects were simulated, such as scratches and plug and epoxy repairs, so that the effect of these conditions could be anticipated.

To obtain data on anode spacing and the current densities, the plating techniques for the large mirror were scaled down for the 4-ft sample. This scaled test provided information on expected edge buildup and thickness uniformity of the nickel plate for the large mirror. The success of this test showed that it was feasible to electroplate nickel onto the 23-ft collimator to the proper specifications.

Although the mirror was nickel-plated in a satisfactory manner, there were several areas in which definite improvements could be made, specifically by attention to detail, procedures and more emphasis on cleanliness.

The poor adhesion of the nickel plate to the extreme OD was probably caused by a low current density during the copper strike or from residual chemicals left in the recess between the polyethylene dam and the mirror face during the various plating steps.

The uniformity of deposition could have been improved by experimentation with anode location and current control. Also, the temperature of the plating solution was not maintained at optimum temperature because the radiative and convective heat losses were greater than the solution immersion heaters could compensate for. A greater development effort in plating large-diameter disks should produce results comparable to that achieved with the 4-ft sample.

D. Grinding and Polishing

The 12-ft ring grinder was used initially to grind off the peaks of variation in the nickel plating. When the plating was ground to the correct figure with minimum defects (which were considered to be capable of removal with a lapping process), the ring grinder was replaced with a 10-ft lapping tool (Fig. 22).

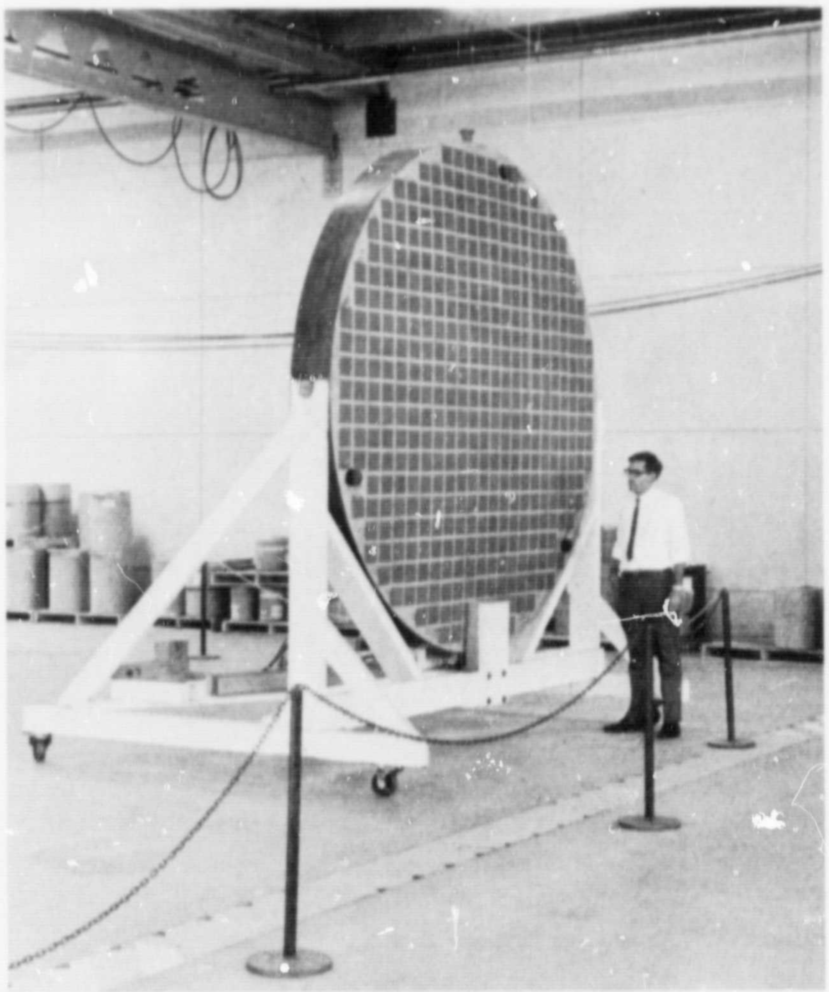

Fig. 22. Lapping tool

The 10-ft lap, which had $4 \times 4 \times 1$-in. cast iron pads attached, was used with successively smaller grit sizes until all imperfections in the nickel plating were removed. It should be noted that some of the tool marks and imperfections, which were thought to have been ground and polished out, were plainly visible when the lap tool worked long enough to produce a specular surface. The removal of material with the lap was a very slow process and all defects should have been worked out previously by grinding. When all the surface defects were worked out with the cast iron lap tool, it was replaced with a 3-ft felt pad tool and a fine polishing abrasive. Polishing with the felt lap continued until all portions of the mirror met the grind and polish optical specifications. Final polishing inspection showed a radius of 1206 in., a total reflectance of the polished nickel of $68 \pm 1.0\%$ and a slope deviation of 10 wavelengths, as measured with a 12-in. diam test glass of the proper curvature and sodium D light. Figure 23 shows the mirror after the polishing was completed and the finished mirror ready for shipment to JPL.

After the mirror was hung in the JPL space simulator chamber, prior to aluminizing, large gray areas in the mirror surface became evident. It was determined that

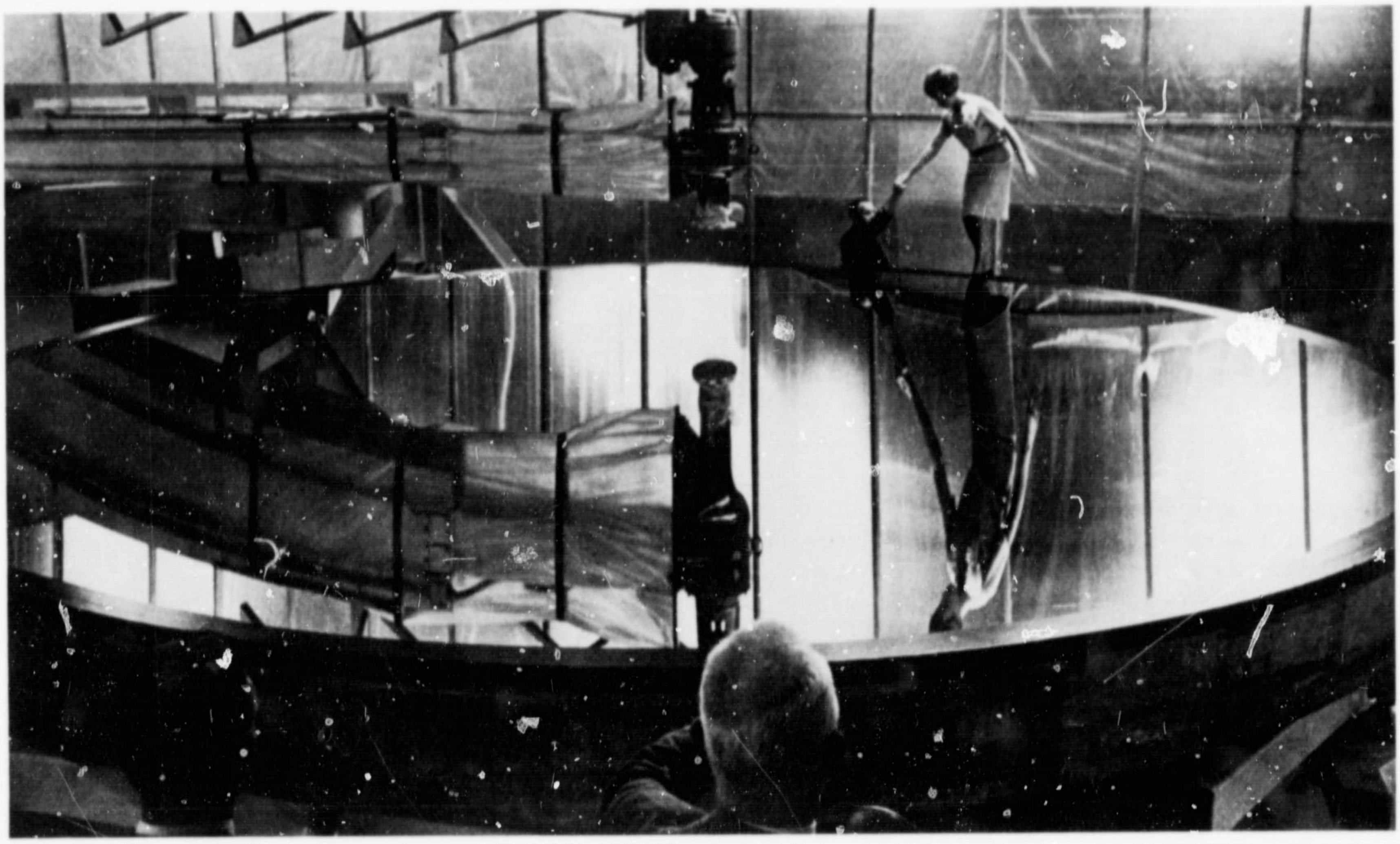

Fig. 23. Mirror after final polishing

these areas had not been polished sufficiently. It was found that the instrument used to detect total reflectivity was not accurate nor sensitive enough to quantitatively detect these gray areas. It is recommended that suitable inspection techniques be developed to describe these conditions and be used to specify mirror surfaces. It is also recommended that the felt lap procedure be eliminated and all polishing be completed with cast iron or pitch lap blocks to obtain a more satisfactory specular surface.

V. Transportation and Installation

Transportation of the large, heavy mirror, which appeared to be a problem early in the project, turned out to be one of the easier phases and to be compatible with existing trucking procedures.

A trunnion support, designed into the mirror structure, allowed the mirror to be lifted and rotated as desired. This trunnion system was originally incorporated to lift the mirror into the chamber, but it was also very useful during all phases of fabrication.

A special handling fixture was designed that adapted the mirror to a hydraulically operated tilt table mounted on a truck. This fixture supported the mirror and protected it against strains introduced by the truck during transit. The tilt table allowed the mirror to ride on the truck in any position, from horizontal to 50 deg above the horizontal. The high angle allowed passage through narrow places, but most of the moves were made in the position shown in Fig. 24.

When the mirror was moved from the metal fabricator to the optical shop, it was merely covered with rubberized canvas to keep out the dirt. Preparation for the shipment of the mirror from the optical contractor to JPL was more involved because the highly polished surface required more protection.

A 60-mil-thick strippable coating (3M-EC-2535) was applied to the polished nickel. The mirror surface was covered with a 10-mil sheet of polyethylene, polystyrene foam bits to fill the hollow of the mirror, a solid 1-in. plywood cover, and a waterproof canvas cover over the entire

Fig. 24. Most commonly used shipping position

assembly. Figure 25 shows the mirror arriving at JPL with its protective covering.

At the construction site, the rigging contractor removed the mirror from the truck and installed it on a six-column support structure designed to allow welding of the prefabricated temperature control manifold to the back of the mirror. The back of the mirror was first cleaned thoroughly with detergents and chemical solutions to remove dirt, grease, and the deposits which had built up over several months on the mirror and temperature control tubes. After cleaning, the mirror was covered with a large 30 × 50-ft air tent. The tent provided an environment suitable for heliarc welding the manifold assembly to the mirror and for helium leak testing the more than 250 separate weld joints (Figs. 26 and 27).

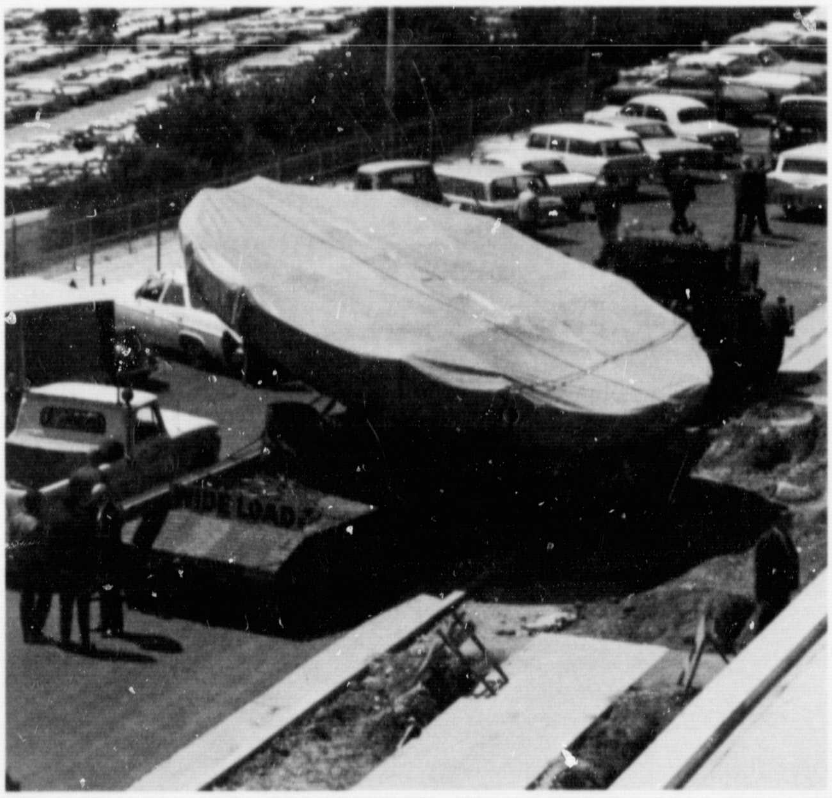

Fig. 25. Mirror arriving at JPL

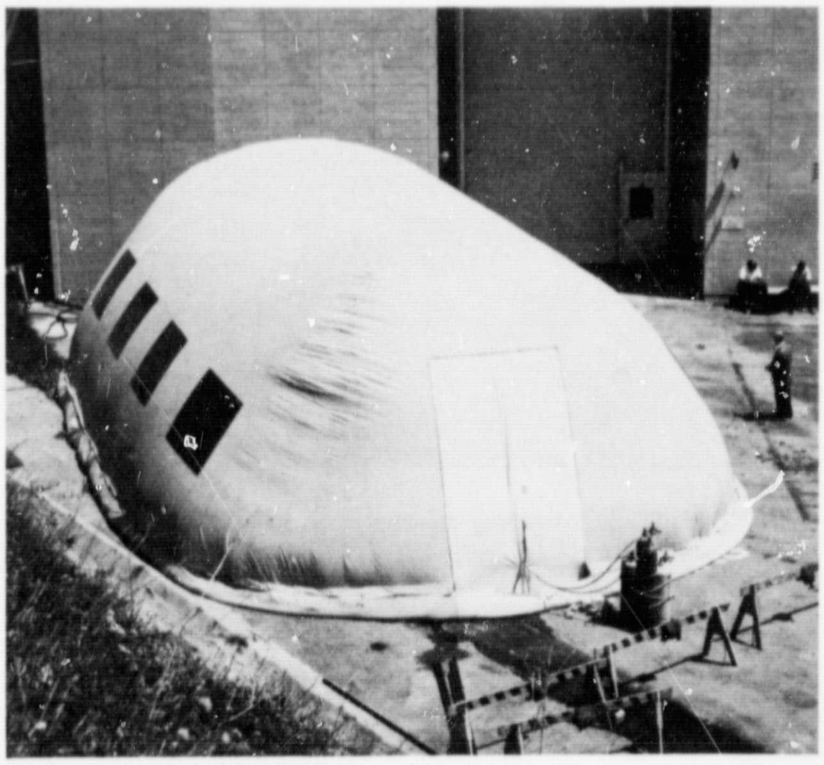

Fig. 26. Air tent

Fig. 27. Heliarc welding tube joints

When all welds were certified leak-tight, the air tent was removed and the mirror was lifted onto a special handling cart (Fig. 28) and moved into the building housing the space simulator (Fig. 29). The mirror was positioned at approximately 60 deg during the trip into the chamber. At the door to the chamber, the mirror was transferred from the cart and crane to the hoisting cables (Fig. 30). The mirror was then lifted into the correct position in the top of the chamber, and its whiffle-tree support and lateral support systems were attached. When the hoisting cables and hardware were removed, a redundant mirror support system was attached to the trunnions, and the mirror was optically aligned and positioned. Final connections of the temperature control manifolds were made to the existing chamber feed-throughs. Finally, the installed temperature instrumentation was hooked up.

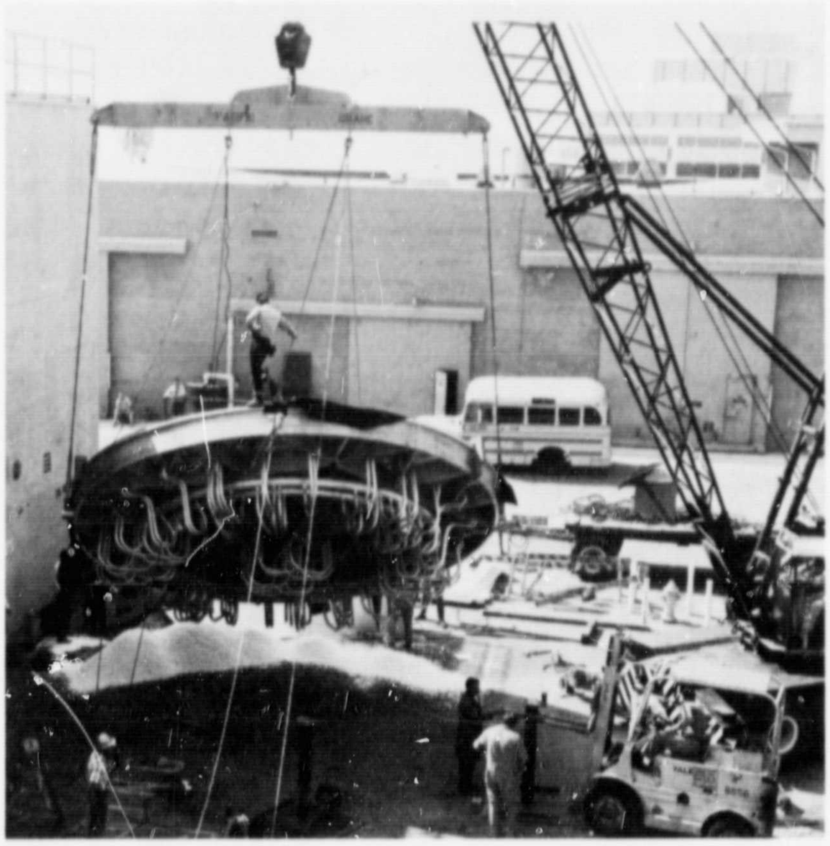

Fig. 28. Moving mirror onto handling cart

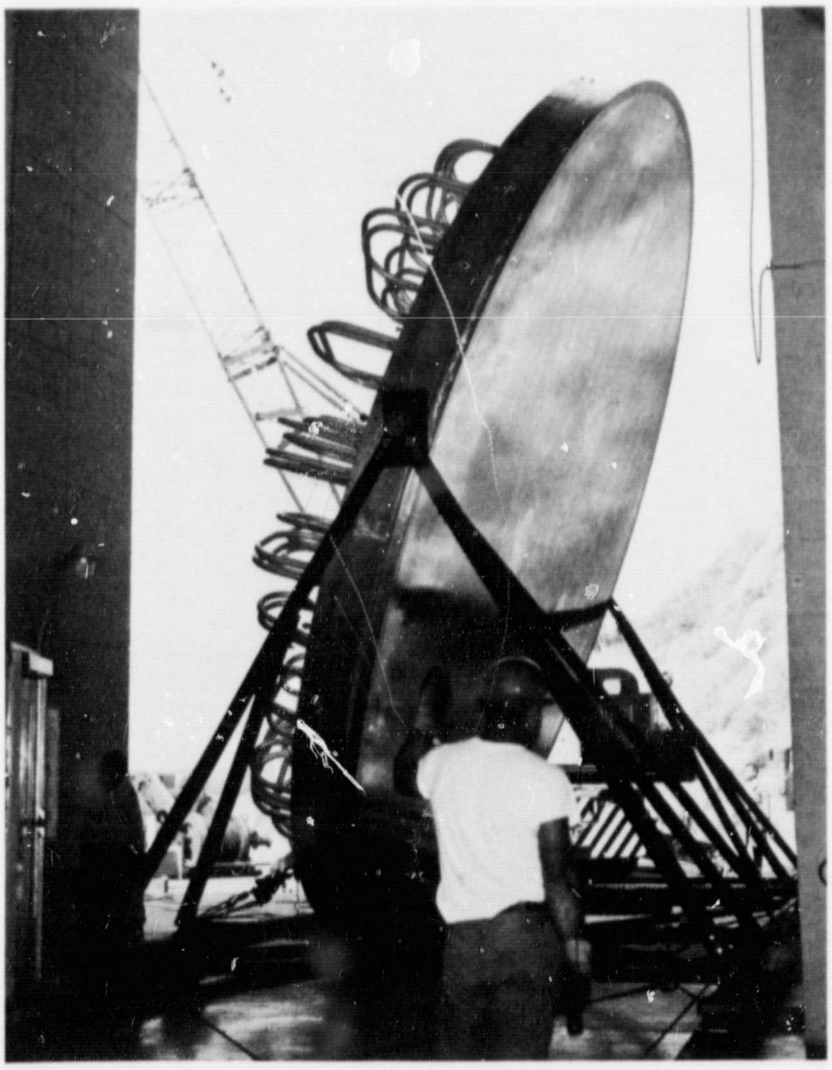

Fig. 29. Moving mirror into building

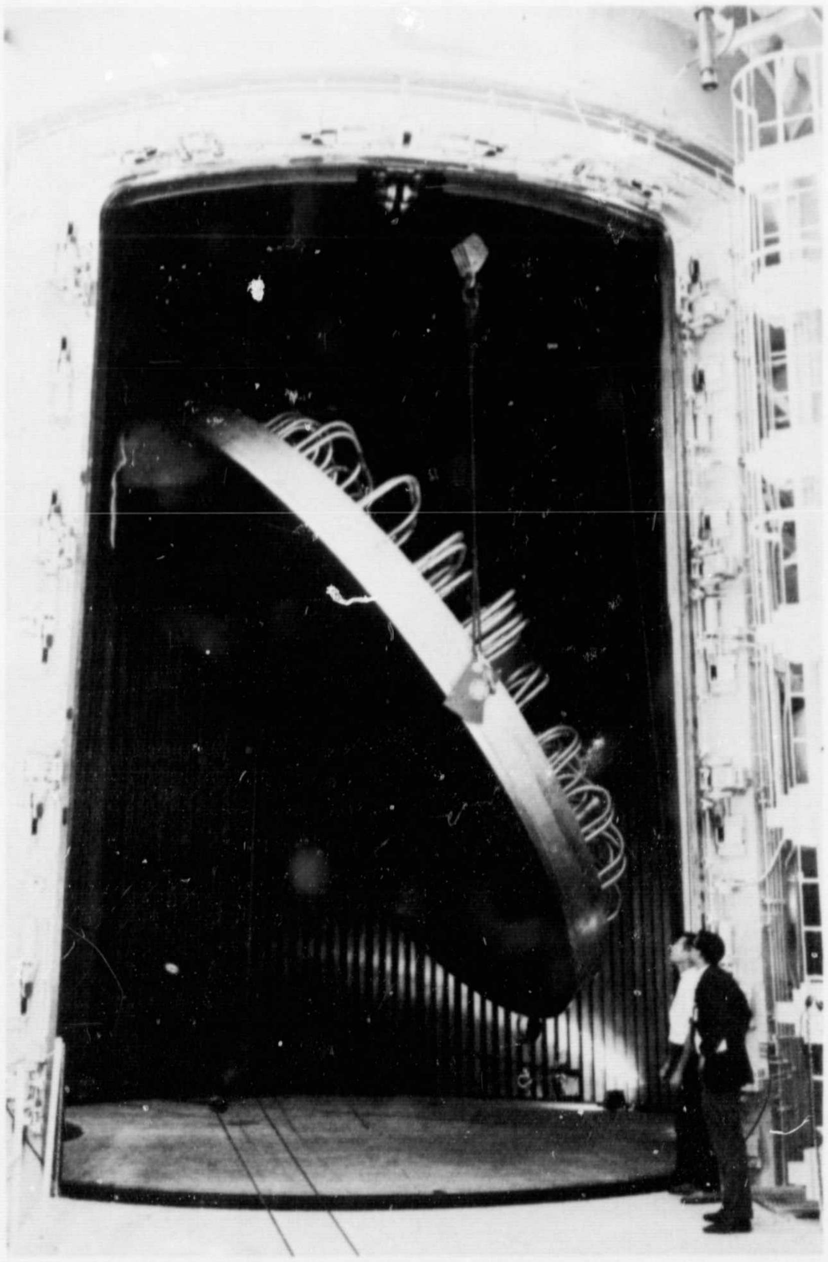

Fig. 30. Mirror on hoisting cables inside chamber

VI. Aluminizing the Mirror

Aluminizing the 23-ft mirror is discussed in detail in Ref. 7. The method chosen was to use a single crucible heated with electron beam guns, rather than 96 double-tungsten filament heaters. The uniformity requirement would have made the tungsten filament vacuum deposition difficult to accomplish, with so many sources.

After the strippable coating was removed from the front face of the mirror, the polished nickel was cleaned with a mixture of aluminum oxide, distilled water, and ethylene glycol. This mixture was allowed to dry and was removed with dry cotton. The mirror was then cleaned by glow discharge in the chamber. The crucible of aluminum was then brought up to temperature by using the three 12-kW electron beam guns and exposed to the mirror front face until the required aluminum thickness was built up.

The vapor deposition occurred at a chamber pressure of 2.5×10^{-5} torr and continued for a period of 38 s from the opening to the closing of the shutters. A precalibrated quartz crystal thickness monitor was used to check the depth of coating, which varied from 1300 Å in the center to 650 Å at the extreme edge and was symmetrically uniform. The total reflectance of the aluminized mirror was 82 ±2% over the entire mirror surface. Although this tolerance was higher than anticipated, it was believed due to the substrate preparation rather than the uniformity of deposition. The nonuniformity due to the slope deviation and mixer distribution was much better than anticipated so that the reflectance tolerance was compensated for.

VII. Conclusions

Large single-piece collimating mirrors of more than 20-ft diam can be fabricated for use in modern, high-quality solar simulators. The aluminum weldment, when properly designed and constructed, will be dimensionally stable and has excellent temperature control characteristics. The mirror reflecting surface can be obtained by electroplating nickel onto the aluminum substrate and figuring and polishing it to a highly specular finish. Vacuum deposition of aluminum on this surface by means of a single-source crucible, heated by electron beams, is capable of producing optimum uniformity of reflectance over the entire mirror diameter.

References

1. Owen, W. A., *Modification of the JPL 25-ft Space Simulator,* Technical Report 32-1273. Jet Propulsion Laboratory, Pasadena, Calif. (to be published).
2. Eddy, R. P., *Design and Construction of the JPL SS15B Solar Simulator,* Technical Report 32-1274. Jet Propulsion Laboratory, Pasadena, Calif. (to be published).
3. Riise, H. N., *SS20B Optical System Ray Trace Using 1620 Computer Program,* Technical Memorandum 33-384. Jet Propulsion Laboratory, Pasadena, Calif. (to be published).
4. Hickman, R. S., *Transient Response and Steady-State Temperature Distribution in a Heated, Radiating Circular Plate,* Technical Report 32-169. Jet Propulsion Laboratory, Pasadena, Calif., Nov. 22, 1961.
5. Batchelder, R. R., and Wada, B. K., *Stiffness Matrix Structural Analysis,* Technical Memorandum 33-75. Jet Propulsion Laboratory, Pasadena, Calif., Feb. 12, 1962.
6. Heilig, M. R., *Nickel Plating of the 23-ft Mirror for the JPL 25-ft Space Simulator,* Technical Report 32-1167. Jet Propulsion Laboratory, Pasadena, Calif., Nov. 1, 1967.
7. Noller, E. W., *Aluminizing the 23-ft Mirror for the JPL 25-ft Space Simulator,* Technical Report 32-1215. Jet Propulsion Laboratory, Pasadena, Calif. (to be published).